CLIMRISK-RIVER: Accounting for local river flood risk in estimating the economic cost of climate change

Predrag Ignjacevic [a,*], W.J. Wouter Botzen [a,c], Francisco Estrada [a,b], Onno Kuik [a], Philip Ward [a], Timothy Tiggeloven [a]

[a] Institute for Environmental Studies (IVM), VU Amsterdam, De Boelelaan 1105, 1081, HV Amsterdam, the Netherlands
[b] Centro de Ciencias de La Atmosfera, Universidad Nacional Autonoma de Mexico, Mexico
[c] Utrecht University School of Economics (U.S.E.), Utrecht University, Utrecht, the Netherlands

ARTICLE INFO

ABSTRACT

This study aims to improve the estimates of the economic impacts of climate change by developing a river flood risk model CLIMRISK-RIVER and introducing it into an existing climate-economy integrated assessment model (IAM). It operates on a local scale and can project climate change-related river flood damage for various socioeconomic, climate and flood adaptation scenarios. Whereas other IAMs have relied on temperature as a climate change proxy, we show that precipitation is a key variable in projecting river flood damage. The way adaptation is accounted for in our flood damage functions has a large influence on the results, highlighting the relevance of modelling local level adaptation in IAMs. Results presented at different spatial scales demonstrate the relevance of river flood damage functions for estimating the economic impacts of climate change and allows for exploration of the spatial distribution of impacts through local estimates.

1. Introduction

Integrated assessment models (IAMs) of climate and the economy are commonly used to project the future economic impacts of climate change. While some IAMs estimate the climate impacts on specific physical systems (eg. energy, land use (Bosetti et al., 2007, Bouwman et al., 2006, Raoet al., 2008)), others paint a more general picture of climate impacts on the economy (Stern, 2008, Nordhaus, 2013, Anthoff and Tol, 2014). The latter set usually provides monetized climate impacts through climate damage functions and/or estimates of benefits of climate policy aimed at reducing the greenhouse gas emissions. Such models estimate the complex relationship between the anthropogenic and climate system using transparent and simplified reduced form functions. Since the original version of the DICE model (Nordhaus, 1992), one of the first IAMs of climate change and the economy, environmental economists have made several attempts to improve these models to aid policymakers in making decisions about climate policy in the face of climate change uncertainty (Tol, 2018).

Nevertheless, climate-economy IAMs have received various criticisms, including the aggregated spatial dimension of the models (Farmer et al., 2015), the incomplete representation of climate change risks

(Stern, 2013), (van den Bergh and Botzen, 2014) and the fact that the damage functions that translate global warming into economic impacts are outdated and require an improvement (Diaz and Moore, 2017). In this respect, it should be noted that in most cases, these IAMs work on an aggregated spatial scale, meaning that there is either one region - the Earth - or several larger regions. For example, the well-known RICE model, which is the regional version of the global DICE model, estimates the economic impacts from climate change for 12 world regions (Nordhaus and Yang, 1996), (Nordhaus, 2017).

Global information about the projected economic impacts of climate change is increasingly available at a refined spatial resolution for specific impact categories, which can serve as a basis for updating the IAM impact functions if this improves IAM estimates of the economic costs of climate change. The effects of extreme weather and natural hazards on the economy due to climate change have been included in climate-economy IAMs to a very limited extent and estimates from catastrophe models of how natural disaster risks are expected to develop under climate change have become increasingly available (Botzen et al., 2019). For instance, river flooding is an important damage category that must be better represented in IAMs, because it poses a significant economic impact, and sophisticated global modelling approaches to
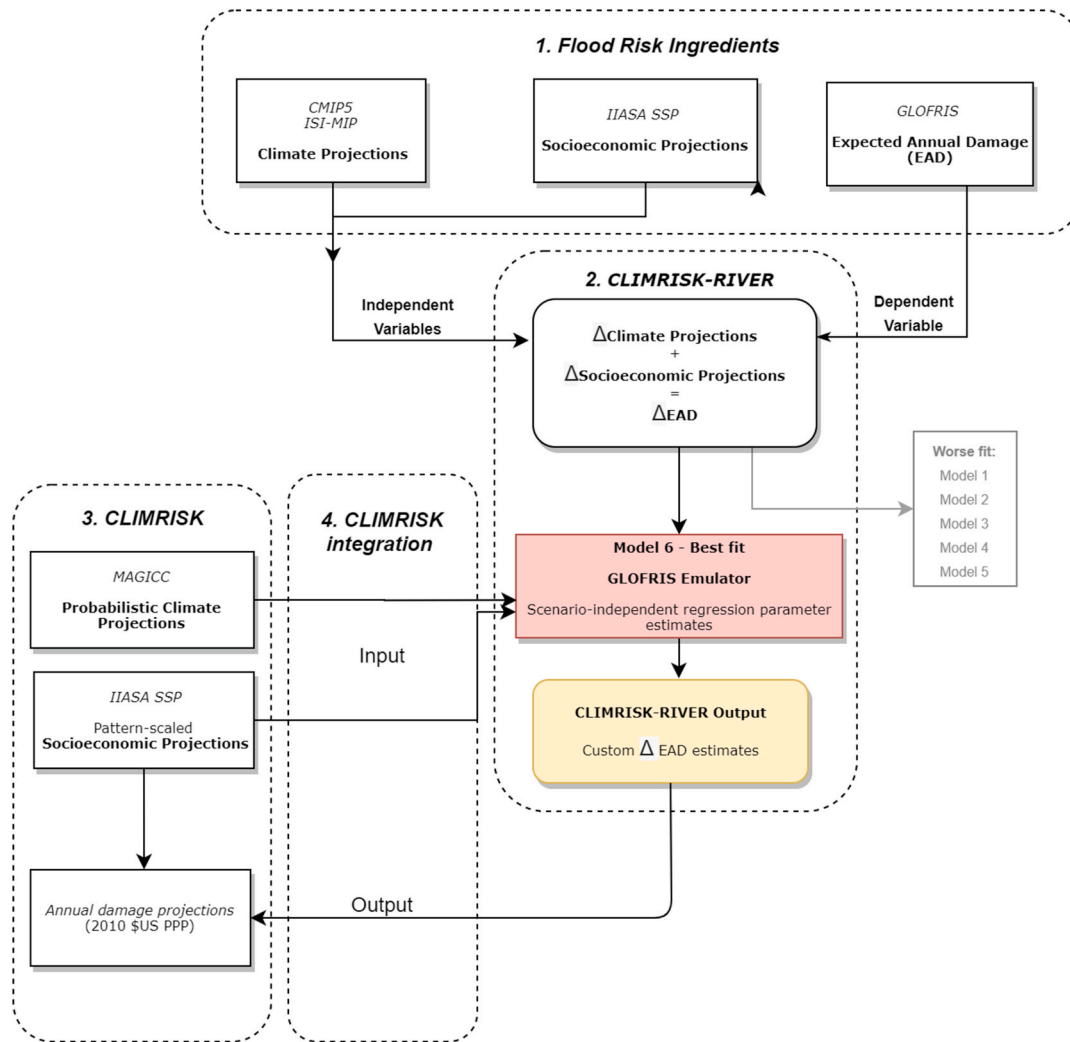
Fig. 1. Structure of the CLIMRISK-RIVER model.

estimate river flood risk at a detailed spatial resolution are increasingly available (Wardet al., 2015). About $ 50 trillion[1] and 0.8 billion people are subjected to a 1-in-100-years river flood event (Kundzewicz et al., 2013) and the direct economic losses from river floods between 1980 and 2013 exceeded $ 1 trillion and caused a loss of more than 220,000 lives (Munich et al., 2014). The river flood risk is expected to increase in many regions in the world (Wardet al., 2013), and it is important to take this into account in economic IAMs of climate change.

The main goal of this paper is to improve the local estimates of the economic impacts of climate change by developing CLIMRISK-RIVER, a spatially-explicit model of river flood risk that is introduced into a broader climate-economy IAM CLIMRISK. There are four main reasons why CLIMRISK is the preferred IAM for this study. First, other IAMs (including RICE) do not provide precipitation projections, which we find to be an important explanatory variable of future changes in flood damages. Second, with CLIMRISK, we can model spatial heterogeneity in climate change impacts. The results of CLIMRISK-RIVER show that spatial heterogeneity in projected flood damages is substantial and modelling this provides insights into which areas face a high river flood risk. Third, CLIMRISK allows us to model climate projections

probabilistically, which gives insights into uncertainty of climate change impacts. Fourth, with CLIMRISK, we are flexible with exploring how climate change impacts develop under many different scenarios, with limited computing time.

CLIMRISK-RIVER also accounts for local human adaptation through the use of recently developed local flood protection standard database FLOPROS (Scussoliniet al., 2016). Accounting for local flood adaptation in estimating the river flood damage functions for the IAM is important as flood protection standards that reduce the probability of a river flooding already exist in many areas in the world. Governments are likely to update these standards if flood risk increases as a result of climate change. Most studies that use IAMs, such as DICE, account for adaptation implicitly through the reduction in the climate damage used in estimating the damage function (Nordhaus, 2017). We follow this approach by estimating the river flood damage functions implicitly using flood damage estimates that account for different flood protection standard scenarios. These scenarios range from maintaining current flood protection standards to implementing economically optimal protection given a climate and socio-economic scenario. Through creating unique flood damage functions under each flood protection scenario, we contribute to the small body of literature that has made adaptation explicit in damage functions in climate-economy IAMs (de Bruin et al., 2009), (Hope, 2011), (Dumas and Ha-Duong, 2013).

---

[1] All units are in US dollars.

Our approach of accounting for river flood risk in a climate-economy IAM is currently the closest to the work of (Kuik, 2017) in introducing the river flood damage functions in the Climate Framework for Uncertainty, Negotiation and Distribution (FUND) model, a climate-economy IAM (Anthoff and Tol, 2014). The flood damage functions in FUND generate estimates for 16 regions as a product of a regional damage coefficient, regional temperature, and gross-domestic product (GDP). Moreover, the functions make use of ad hoc medium and high adaptation scenarios from (Jongman et al., 2015). However, with gridded flood damage and flood protection standard data available, it is now possible to produce accurate local estimates of expected annual flood damage. CLIMRISK-RIVER flood damage functions are spatially more detailed; more complete, as they account for wet and dry regions by means of gridded precipitation projections as an additional explanatory variable; and have a more realistic representation of adaptation policy. The reason for the latter is that flood adaptation scenarios are not implicitly assumed, but are modelled using data on existing, and future, economically optimal flood protection standards (Scussolini et al., 2016), (Ward et al., 2017).

The end product of CLIMRISK-RIVER is a set of flood damage function estimates which are introduced into a general framework of CLIMRISK, which allows the user to explore climate change related damage, including the expected damage due to river flooding. The model works for any user defined climate change and socioeconomic scenario combination presented in the IPCC 5th assessment report. The model can be used by policymakers interested in expected future changes in flood risk and implementing a flood adaptation policy in a particular geographic area. For this audience, CLIMRISK-RIVER can serve as a preliminary quick scan that gives insights into how flood risk is expected to develop under future scenarios and the effectiveness of flood protection infrastructure to limit this risk, which can be a motivation for conducting additional higher resolution studies to identify appropriate local flood risk management measures. Other users are members of the academic community who are interested in mapping river flood hotspots under different future scenarios to motivate further local-scale flood adaptation or climate hazard research. Moreover, the integration of flood risk in a general climate-economy IAM is likely to appeal to the broader community of researchers and policymakers who are interested in understanding global, regional, or local economic impacts from climate change.

2. Methodology and data

In this section, we present the methodology used to develop CLIMRISK-RIVER. This section follows a downstream flow that resembles the flow of methods presented in the flowchart Fig. 1. Firstly, we outline the ingredients required for developing the new river flood damage functions that emulate GLOFRIS (subsection 2.1). Next, we develop 6 regression models and evaluate their performance based on in-sample and out-of-sample GLOFRIS data (subsection 2.2). Once the most suitable model - Model 6 - is selected, it is introduced into the CLIMRISK model by feeding it downscaled climate and socioeconomic data from a spatially explicit IAM CLIMRISK (explained in Appendix subsection A). Finally, the results of CLIMRISK-RIVER and the resulting total climate damage of CLIMRISK after integration are presented in Section 3.

2.1. Flood risk ingredients

The main goal in developing CLIMRISK-RIVER is to produce validated river flood damage functions for different protection standard assumptions that can be fed with temperature, precipitation and GDP estimates from any climate or socioeconomic scenario combination. The input for the flood risk emulator CLIMRISK-RIVER is based on the GLOFRIS model, a global framework for flood risk assessment that works on a detailed spatial scale (30" × 30") and includes all main river basins

worldwide (Winsemius et al., 2012). The main ingredients of the new flood damage functions for CLIMRISK-RIVER are as follows:

- **Risk:** Expected annual damage (EAD)
- **Vulnerability:** Flood protection standards
- **Hazard:** Climate projections
- **Exposure:** Economic projections

Each of the above listed ingredients are explained in more detail in the following sections.

2.1.1. Risk: expected annual damage (EAD)

Formally, flood risk can be defined as the expected annual damage (EAD) or the damage of a hazardous event weighted by the probability of its occurrence. Over a smooth probability curve, it can be written as:

$$EAD = \int_0^1 pD(p)dp \tag{1}$$

where EAD represents the EAD of the particular cell, $D(p)$ is the damage in that cell caused by a flooding event of probability p, which is related to a flooding with return period $r(p)$ in the following way:

$$r(p) = \frac{1}{p} \tag{2}$$

The EAD estimates are made using current and future flood hazard layers, built-up area, GDP estimates, country level maximum damage estimates and depth-damage curves based on the occupancy type (Ward et al., 2017), (Tiggeloven et al., 2020), (Winsemius et al., 2016).

To estimate the flood damage functions for CLIMRISK-RIVER using GLOFRIS data, we must retrace the steps of how the data were created in the first place. In GLOFRIS, flood damage is estimated for flood return periods of 2, 5, 10, 25, 50, 100, 250, 500 and 1000 years. For illustration, the damage of a 2-year return period represents the loss that would be caused by relatively small floods with annual exceedance probability of 0.5. The resulting flood probabilities were calculated using Equation (2) and a smooth probability curve was obtained for the purpose of EAD estimation between the above-mentioned points. The EAD in CLIMRISK-RIVER for any particular cell can be calculated using the trapezoidal rule for approximating definite integrals:

$$EAD_{GF} = \sum_{i=1}^{10000} \frac{D_{GF}(x_{p-1}) + D_{GF}(x_p)}{2} \Delta x_p \tag{3}$$

where EAD_{GF} is the approximation of EAD (Eq. (1)) in the GLOFRIS (GF) model, $x \in [0,0.0001 \dots,1]$ is a vector of equally spaced 10,000 points and $\Delta x_p = \Delta x$ is the length of equal spacing.

These loss data are estimated in GLOFRIS for current conditions, but also for future climate and socioeconomic scenarios, and are available for different time periods centered around three years: 2030, 2050 and 2080. The GLOFRIS modelling cascade uses forcing data from EU-WATCH (Weedon et al., 2011) over the period of 1960–1999 to force the hydrological model PCR-GLOBWB (Sutanudjaja et al., 2018) which is used for the flood inundation modelling as baseline conditions. As baseline for the socioeconomic data, GLOFRIS uses the HYDE database, which consists of gridded percentages of built-up area, population and GDP projections.

As a starting point, damage estimates for rivers of different return periods for the baseline period are collected and these do not depend on different emissions or socioeconomic scenarios. Hence, the baseline represents current climate and socioeconomic conditions. The future projections of flood damage, however, are available for various climate[2]

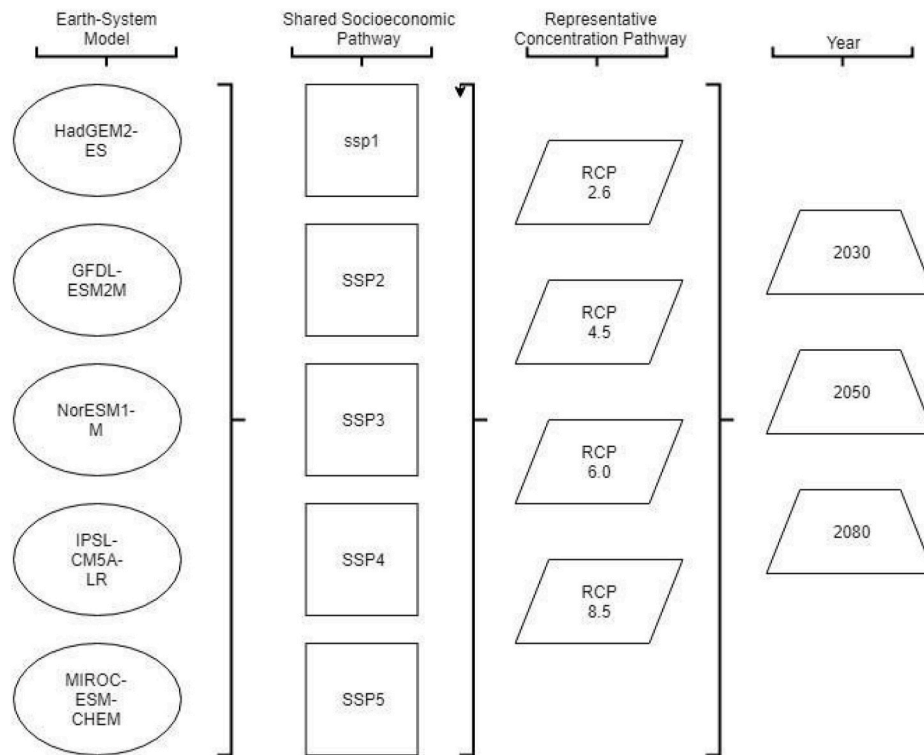[2] Climate scenarios: RCP2.6, RCP4.5, RCP6.0, RCP8.5.

Fig. 2. All possible future scenario combinations of flood damage data used to generate the flood damage functions.

and socioeconomic scenarios.[3] Finally, the data are available for five different earth system model (ESMs)[4] simulations that were used to force the GLOFRIS model projections for each RCP scenario (see Fig. 2). Each of the above-mentioned combinations of climate and socioeconomic scenarios for different ESMs in different time periods produces a single observation of EAD for each cell. Therefore, each cell ideally contains 305 observations of EAD with no missing data.[5] By pooling estimates from different ESMs in our damage function estimation, we are effectively averaging across all five available ESMs and making our emulator ESM independent. With respect to climate input, the user would only need to specify the RCP scenario and global average temperature percentile realization through MAGICC (Appendix A.1), which would naturally correspond to a particular ESM.

All the EAD estimates are expressed in billions of US dollars (2005 PPP) and are available for $30'' x30''$ cells. To integrate CLIMRISK-RIVER into the CLIMRISK model, all the GLOFRIS river flood data must be upscaled to $0.5° \times 0.5°$ by aggregating the impacts over the $30'' \times 30''$ cells. Prior to integration with CLIMRISK-RIVER, the emulated damage estimates were translated into US dollars (2010 PPP) to match the CLIMRISK monetary impact estimates when providing the total climate-change damages.

2.1.2. Vulnerability: flood protection standards

To obtain more reliable estimates of annual expected river flood damage, the current flood protection standards must be taken into

account. The flood protection standards enter the flood risk model through the EAD function whereby damages of rivers with return periods lower than the available protection standards are assumed to be zero. For example, if an area is protected against a 500 year return period flood, this means that the sum in Equation (3) only contains damage estimates of rivers with return periods greater than 500 years.

A comprehensive global database - FLOPROS - of observed and modelled current river protection standards has recently been compiled (Scussoliniet al., 2016). The flood protection data are available at the state level and any given cell receives protection equal to its estimated state protection level. The river protection data are currently available for 2683 states in the world in the form of river return periods against which the state is protected. However, in estimating the annual expected flood damage in the future, we also need estimates of future flood protection standards that depend on adaptation decisions about flood protection investments. FLOPROS data consists of two options for future protection standards[6]

- *Baseline Height Standards (BaseHeightStd)*, which assume that the protection infrastructure is maintained at the baseline year *height* in the future and allow the river flood risk to vary over the course of the century. This scenario does not imply any additional river flood adaptation.
- *Baseline Probability Standards (BaseProbStd)*, which assume that the protection standards are updated so as to keep the baseline flood probability constant. This scenario does imply additional river flood adaptation as the flood protection standards are upgraded according to the varying natural factors in order to maintain constant flood

---

[3] Socioeconomic scenarios: SSP1, SSP2, SSP3, SSP4, SSP5.

[4] ESMs used: HadGEM2-ES, GFDL-ESM2M, NorESM1-M, IPSL-CM5A-LR and MIROCESM-CHEM.

[5] The number 305 comes from the fact that there are $5ESMs \times 5SSPs \times 4RCPs \times 3years = 300$ plus 5 additional baseline period observations (for each ESM).

[6] The names assigned to the protection standards in this paper are arbitrary and do not correspond to the names given by the original authors of the flood protection standards.

probability. Regardless of the constant flood probability, the flood-related damage could still vary with the amount of exposed assets and the severity of flooding.

Taking this research a step forward through cost-benefit analysis, policymakers' desired economic decision-making has been taken into account when designing the optimal level of river flood protection (Kuik, 2017).

- *Optimal Standards (OptimalStd)*, which assume that all states behave in an economically optimal manner and invest today in the level of protection that would yield the highest net present value (NPV) over the twenty-first century.

In addition to the three adaptation scenarios, a fourth scenario - *No Standards (NoStd)* - will be used for comparison with the other assumptions. As suggested by the name, this scenario assumes that no cells are protected against any potential river floods, thereby ignoring existing protection standards as modelled in FLOPROS. This is true for both the baseline year estimates and future projections. Although this is not a very realistic assumption, it helps us understand how important flood protection standards are in estimating the flood damages in an IAM.

The data for optimal protection standards is not available for some cells due to, for example, missing future projections of socioeconomic data. In such cases, we assume that the protection is maintained at the *BaseHeightStd* level (if available).

2.1.3. Hazard: climate change projections

As in many climate IAMs, annual surface air temperature is among the primary climate variables of interest and serves as the main proxy for climate change. We are also interested in the effect of annual precipitation on the river flood risk. Precipitation has, until now, not been introduced into an IAM damage function and it is important to assess its impact on river flood risk in light of newly available local precipitation data. Although floods are generally short-lived events that are mainly driven by extremes in precipitation, we follow the common approach in IAMs to use annual climate indicators (in our case annual temperature and precipitation) as a proxy of climate change. This is in line with the purpose of CLIMRISK-RIVER to project changes in long term annual expected flood damage in response to long term trends in economic exposure and climate change, which as our results show can be approximated by changes in annual temperature and precipitation (Section 3.1).

Whereas the climate forcing data in CLIMRISK is generated through MAGICC with the use of pattern scaling (see Appendix A.1), the forcing data in GLOFRIS contains daily gridded estimates of surface temperature and precipitation. These are generated using different ESMs, interpolated to $0.5° \times 0.5°$, and they are bias corrected using observations from 1960 to 1999 for the EU-WATCH project. These same estimates are then used to force the PCR-GLOBWB global water and hydrological model (Sutanudjaiaet al., 2018). The EU EU-WATCH forcing observations are also used to generate the baseline flood risk. The reason why 2010 is not used as the baseline period for the climate forcing data in GLOFRIS is the fact that the authors used a 40-year interval around the year of interest in extreme value analysis. As observed data is not available for 1990–2030, the authors assume that global hydrological processes did not drastically change between 1980 and 2010 after accounting for climate. Therefore, the EU-WATCH baseline period estimates are used in the year 2010 as the baseline period. To create the climate input variables necessary for the river flood damage functions, daily temperatures were converted to annual mean temperature and daily precipitation to total annual precipitation. Since the GLOFRIS model produces estimates for three periods centered around years 2030, 2050 and 2080, mean annual surface temperature and total annual precipitation estimates were averaged over the years 2010–2050, 2030–2070 and 2060–2100. Finally, differences of precipitation and temperature with respect to the

baseline period average climate were taken in order to fit the MAGICC climate projection units. For temperature, the difference is expressed in absolute value of degrees Celsius, while for precipitation the percentage change of precipitation with respect to baseline period is required.

2.1.4. Exposure: economic projections

Exposure is another important determinant of flood damage, because it captures the extent of assets that are prone to flooding. GDP PPP was extracted from the SSP-database with the OECD Env-Growth GDP projections. The GDP data used to estimate the flood damages in GLOFRIS are derived from the IIASA SSP Database (Riahiet al., 2017). Next, the future development of urban areas is estimated using the 2UP model (Van Huijstee et al., 2018). In this model, urban and rural populations are distributed according to a map of urban areas, which helps in determining the exposure of a certain area. In CLIMRISK-RIVER, we proxy the GLOFRIS exposure data using IIASA projections for various SSP scenarios combined with the compatible SRES scenarios to create a spatially explicit, $0.5° \times 0.5°$ grid of local GDP estimates. More information about exposure, SSP and SRES data can be found in Appendix A.2.

2.2. CLIMRISK-RIVER

An important step in CLIMRISK-RIVER development is the formulation of the flood damage functions. The main decisions involved in this step are:

- Geographic scale of model parameters
- Choice of explanatory variables

The geographic scale of model parameters refers to the geographic area that a particular damage function coefficient covers. Depending on input data availability, the scale can range between highly local 30" × 30" grid cells and global. Since the scale of downscaled inputs in our IAM is somewhere in between, the primary candidates for the model scale in CLIMRISK-RIVER are the $0.5° \times 0.5°$ grid cell and river basin level. The main advantage of river basin level functions is simplicity - each cell within a river basin would inherit the set of parameters corresponding to the basin. The main disadvantage, however, is the loss of model fit as heterogeneous grid cell data are aggregated into a single function over a potentially large basin area. The opposite is true of a grid cell level function. As we prefer the higher explanatory power of the grid cell level functions over the smaller total number of function estimates, we set the scale to grid cell level to make full use of local input data. The scale of results is still entirely up to the user who can explore various scenario combinations at different levels of aggregation.

The next step concerns the choice of the dependent and explanatory variables. The main goal of the regressions that follow is to project the ΔEAD_t, that is, the change in EAD with respect to the baseline period. For the available data, t represents a time period mid-point for which the GLOFRIS expected annual damage estimates are made, namely, $t \in [2010, 2030, 2050, 2080]$.

In order to find the most suitable statistical model for CLIMRISK-RIVER, we take a nested model approach and evaluate several functional forms with increasing number of terms.

The following nested model consisting of six functional forms is evaluated:

Model 1: $\Delta EAD_{GF,t} = \beta_1 \Delta GDP_t$
Model 3: $\Delta EAD_{GF,t} = \beta_1 \Delta GDP_t + \beta_2 \Delta T_t$, where ΔT_t represents the absolute change in annual mean surface air temperature in year t[7]
Model 3: $\Delta EAD_{GF,t} = \beta_1 \Delta GDP_t + \beta_2 \Delta T_t + \beta_3 \Delta T_t^2$

---

[7] All changes in temperature and precipitation are with respect to 1980 observed climatology from EU-WATCH (Weedonet al., 2011).

Model 4: $\Delta EAD_{GF,t} = \beta_1 \Delta GDP_t + \beta_2 \Delta T_t + \beta_3 \Delta T_t^2 + \beta_4 \Delta P_t$, where ΔP_t represents the percentage point change in precipitation in year t.
Model 5: $\Delta EAD_{GF,t} = \beta_1 \Delta GDP_t + \beta_2 \Delta T_t + \beta_3 \Delta T_t^2 + \beta_4 \Delta P_t + \beta_5 \Delta P_t^2$

Model 6: $\Delta EAD_{GF,t} = \beta_1 \Delta GDP_t + \beta_2 \Delta T_t + \beta_3 \Delta T_t^2 + \beta_4 \Delta P_t + \beta_5 \Delta P_t^2 + \beta_6 \Delta T_t \Delta P_t$, where $\Delta T_t \Delta P_t$ represents the interaction term between temperature and precipitation change.

After evaluating the six different emulator models, Model 6 proved to have the best predictive power across different RCP-SSP scenario combinations. In other words, Model 6 presents the best emulator of our chosen river flood risk model GLOFRIS and is chosen as the **CLIMRISK-RIVER model**. It is defined as:

$$\Delta EAD_{GF,t} = \beta_1 \Delta GDP_t + \beta_2 \Delta T_t + \beta_3 \Delta T_t^2 + \beta_4 \Delta P_t + \beta_5 \Delta P_t^2 + \beta_6 \Delta T_t \Delta P_t \tag{4}$$

where β_1 is the effect of a \$1 billion increase in GDP,[8] ΔGDP_t is the difference in GDP between year t and 2010, β_2 is the effect of a 1 °C increase in surface air temperature, ΔT_t represents the change in mean surface air temperature at t, β_3 is the squared term of surface air temperature, ΔT_t^2 is the change in squared surface air temperature at t, β_4 is the effect of a 1% increase in total annual precipitation, ΔP_t is the percentage point change total annual precipitation at t, β_5 is the squared term of total annual precipitation, ΔP_t^2 is the percentage point change in total squared annual precipitation at t, β_6 is the effect of a 1% increase in total annual precipitation conditional on a 1 °C increase in surface air temperature and $\Delta T_t \Delta P_t$ is the interaction term between the change in mean surface air temperature and the percentage point change in mean total annual precipitation at t.

This model was selected so as to take advantage of the explanatory power of precipitation when estimating ΔEAD. Precipitation could capture the effect that wetter (or drier) regions could have on the frequency of flooding. In addition, the interaction between temperature and precipitation could capture the interaction between, for example, hotter and wetter regions both of which could lead to an increase in flood risk higher than estimated by temperature and precipitation alone. This functional form is similar to the functional form of the RICE damage function, where quadratic climatic terms are used to capture nonlinear effects on damage of high temperature and in our case also precipitation that is excluded in RICE (Nordhaus, 2014). There is no constant term in the regression as the function passes through the origin, and the left and right-hand side terms are zero in the baseline year. While the *GDP* estimate in RICE is multiplied by the impact function (Eq. (11)), the ΔGDP_t in this model is an explanatory variable. The specific units for temperature and precipitation explained above were selected so as to match the MAGICC model output (Appendix A.1). MAGICC generates differences in annual surface temperature in degrees Celsius and percentage difference in annual precipitation with respect to any particular base year. Since the precipitation data used for the fitting was originally expressed in $\frac{kg}{m^2*s}$, a unit conversion is necessary to obtain the percentage difference:

$$\Delta P_t = 100 * \frac{P_t - P_0}{P_0} \tag{5}$$

where ΔP_t is the percentage change in total annual precipitation in year t, P_t is the total annual precipitation estimate at time t, and P_0 is the baseline total annual precipitation estimate.

Due to the large number of possible scenario combinations that can be fed to the CLIMRISK-RIVER model, a select few are presented in this paper. As climate and economic trajectories are uncertain, it is useful to consider the "middle-of-the-road" case of either flood risk driver and to explore the impact of varying the other. In this paper, we chose to keep the socioeconomic aspect of development fixed by opting for the SSP2

Table 1
Comparison of average Adj.R2 across different CLIMRISK-RIVER model candidates.

Average Adj. R^2	*NoSTD*	*BaseProbSTD*	*BaseHeightSTD*	*OptimalSTD*
Model 1	0.57	0.62	0.44	0.37
Model 2	0.64	0.69	0.52	0.48
Model 3	0.66	0.71	0.56	0.57
Model 4	0.74	0.77	0.66	0.63
Model 5	0.75	0.78	0.67	0.64
Model 6	0.76	0.78	0.69	0.66

scenario. Therefore, we vary the climate projection and mainly focus on the following two scenario combinations [9]

1. *Unsustainable World in the Middle of the Road (RCP6.0 - SSP2):* In this scenario, the carbon emissions peak around year 2080, declining thereafter. In combination with the SSP2 scenario of intermediate challenges for both adaptation and mitigation, this scenario combination allows us to explore the impact of an intermediate baseline scenario without any emission reduction policies.
2. *Sustainable World in the Middle of the Road (RCP2.6 - SSP2):* "Abiding by the Paris Climate Agreement (RCP2.6) and strongly curbing carbon emissions (well below 2 °C) this scenario is consistent with the sustainable future assumption whereby countries are abiding by the Paris Climate Agreement (Schleussner et al., 2016).

Given these two contrasting representations of carbon emission development, expected economic damages from not mitigating climate change to 2 °C can be calculated. In addition, we will also compare SSP1 and other SSPs in the Results section to explore the uncertainty arising from economic development. Since the model can project annual damages up to 2100, it is common practice to calculate the net present value (NPV) of those damages using a discount rate (Tol, 2008). This estimate is referred to as discounted climate damages. This rate is set at 3% as is common in other IAMs (Tol, 2018), (Nordhaus, 2017). Therefore, whenever we refer to discounted total ΔEAD, we are, in fact, referring to the change in total EAD in a particular area in the twenty-first century between the years 2010 and 2100, discounted at 3% annually.

After the proposed Model 6 is selected as the CLIMRISK-RIVER model, the next step is to introduce it into CLIMRISK in the following manner (see Appendix A):

1. MAGICC model is used to generate probabilistic estimates of global temperatures for the period 2010–2100.
2. CLIMRISK's pre-defined downscaling factors for each cell are used to obtain grid-cell level annual mean temperature and precipitation data.
3. The downscaled MAGICC climate and SRES/IIASA socio economic data is fed to the CLIMRISK-RIVER damage function to obtain grid cell level river flood damage estimates.
4. The absolute expected river flood damage is added to the CLIMRISK damage estimates, making up the improved CLIMRISK estimate of climate-related damages.

In the following section, the expected river flood damage estimates of the CLIMRISK-RIVER are presented first, followed by the total expected climate-related damage from the integrated CLIMRISK model.

---

[8] All the listed effects refer the change in expected flood damage ΔD_t.

[9] In addition to these two consistent climate-economy scenarios, we also present some results for other RCP scenarios when we explore the advantages of climate change mitigation in Section 3.2.
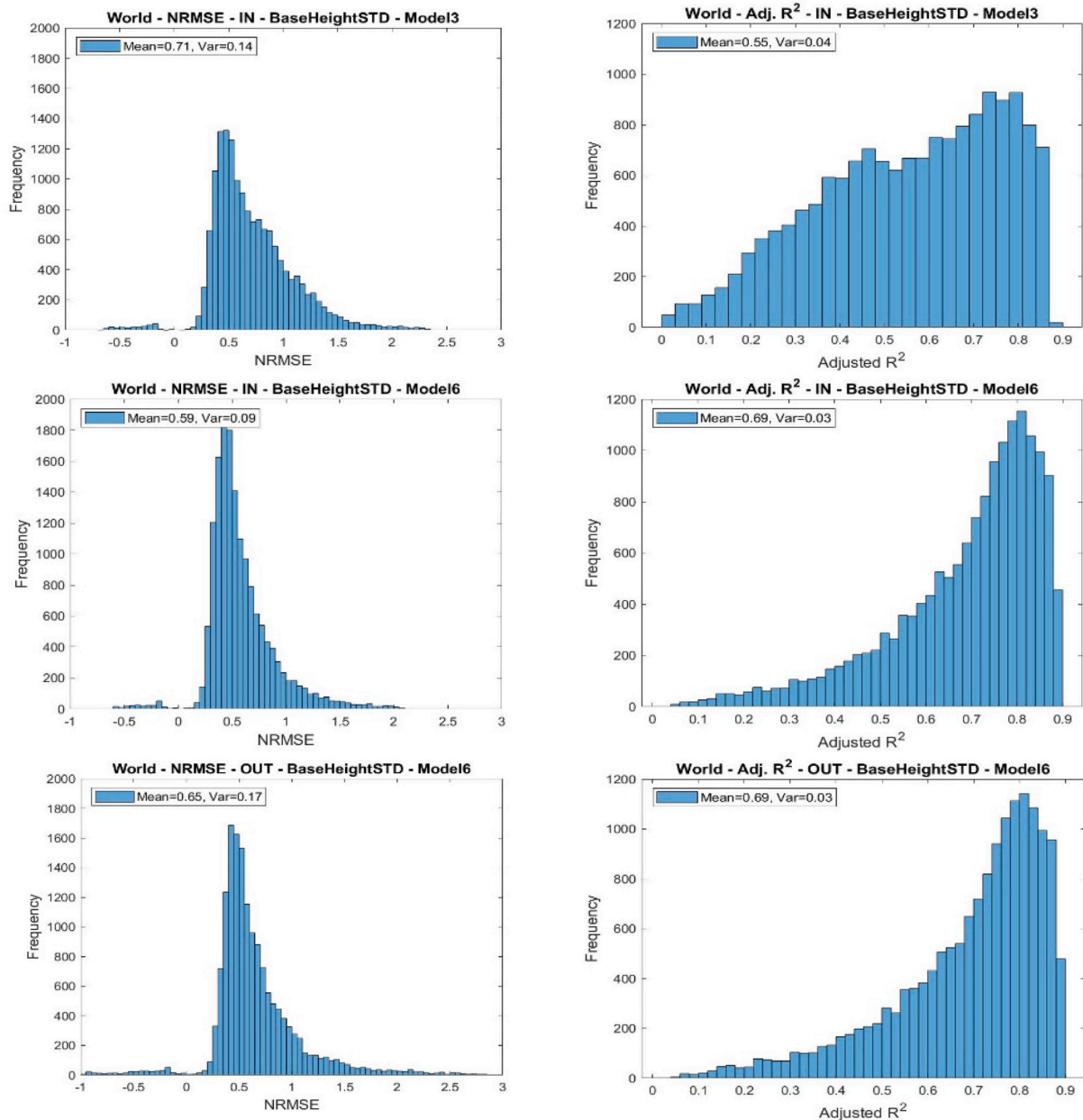
Fig. 3. In-sample (IN) and out-of-sample (OUT) model fit and forecasting performance of Models 3 and 6. There is no evidence of over-fitting as there is little difference between the NRMSE and adjusted R2 distribution of IN (row 2) and OUT (row 3).

3. Results

In this section, we present some key results from the CLIMRISK-RIVER model. First, the model is validated using in-sample and out-of-sample ΔEAD estimates from the original GLOFRIS model. Next, the flood damage estimates produced by the CLIMRISK-RIVER model are presented on an aggregate level for several large regions in the world. Here, we also present some key country-level results. Finally, particularly interesting local damage estimates are presented to illustrate the relevance of estimating climate impacts at a spatially explicit level. Here we specifically focus on grid cells most affected by river flooding and identify cities that fall under these areas in the world and in Europe.

3.1. CLIMRISK-RIVER model evaluation

The performance of the climate change related river flood damage functions must first be evaluated before being introduced into the

CLIMRISK framework. First, we evaluate the adjusted R^2 value for each model across all grid cells to see how much of the variation in ΔEAD it can explain. Next, we evaluate the in-sample and out-of-sample forecasting performance of the model by computing the mean-normalized root mean squared error (NRMSE) for each cell.[10] The results in the main text focus on two protection standard assumptions, *BaseHeightStd* and *OptimalStd*, which were selected because of the need to capture the most realistic range of adaptation policies focused on maintaining the current height of flood protection (*BaseHeightStd*) and moving towards protection standards that are economically optimal given socio-economic development and climate change (*OptimalStd*). The *NoStd* assumption can lead to misleading flood risk predictions and is used solely to illustrate the importance of including flood protection

---

[10] See Appendix C.1 for the description of NRMSE and Appendix C.2 for more NRMSE results.
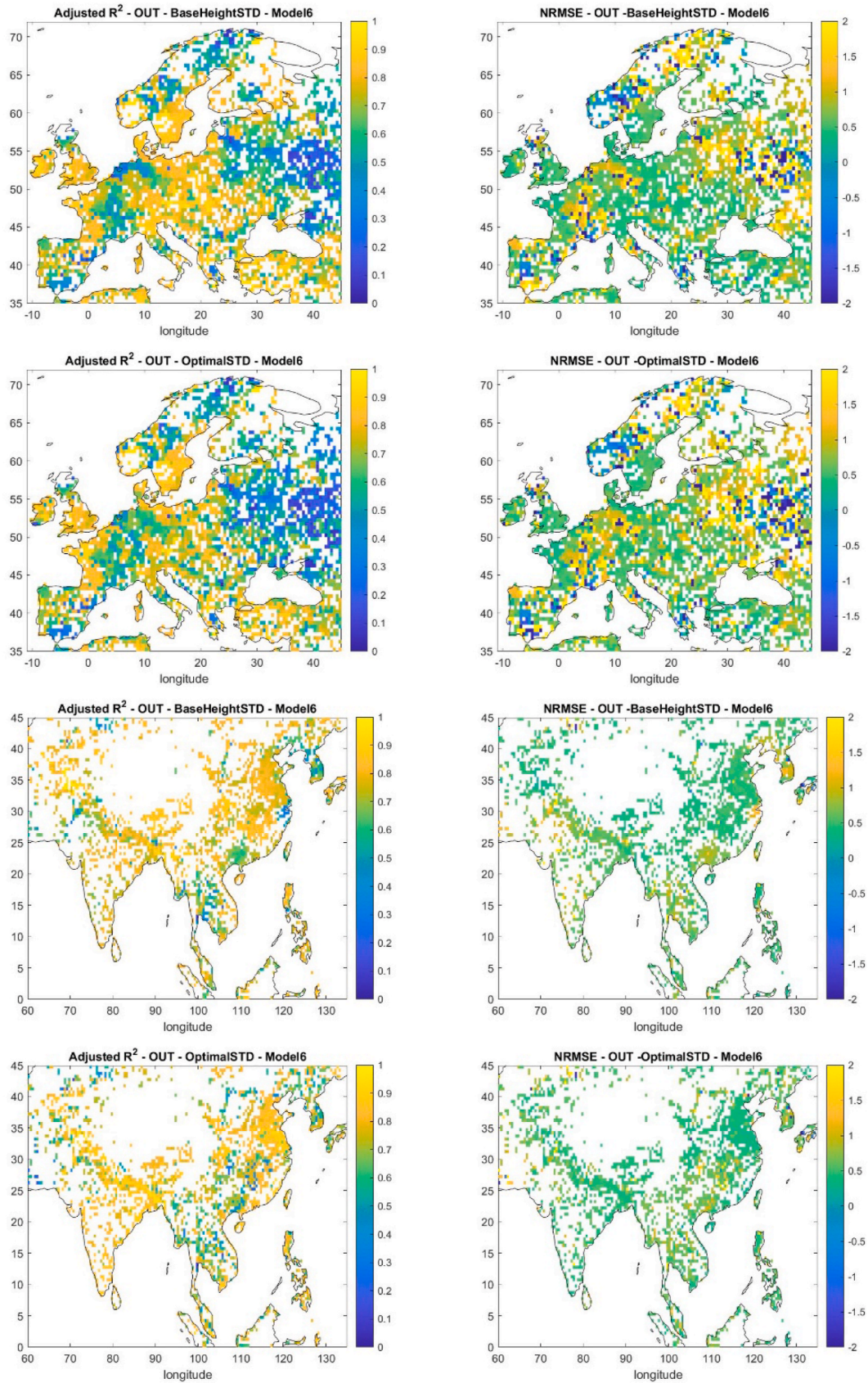
Fig. 4. Adjusted R2 and NRMSE: Measures of model fit and forecasting performance in Europe and South-East Asia. When NRMSE = 1 for a given cell, the model makes a forecasting error equivalent to one mean value of the observations.
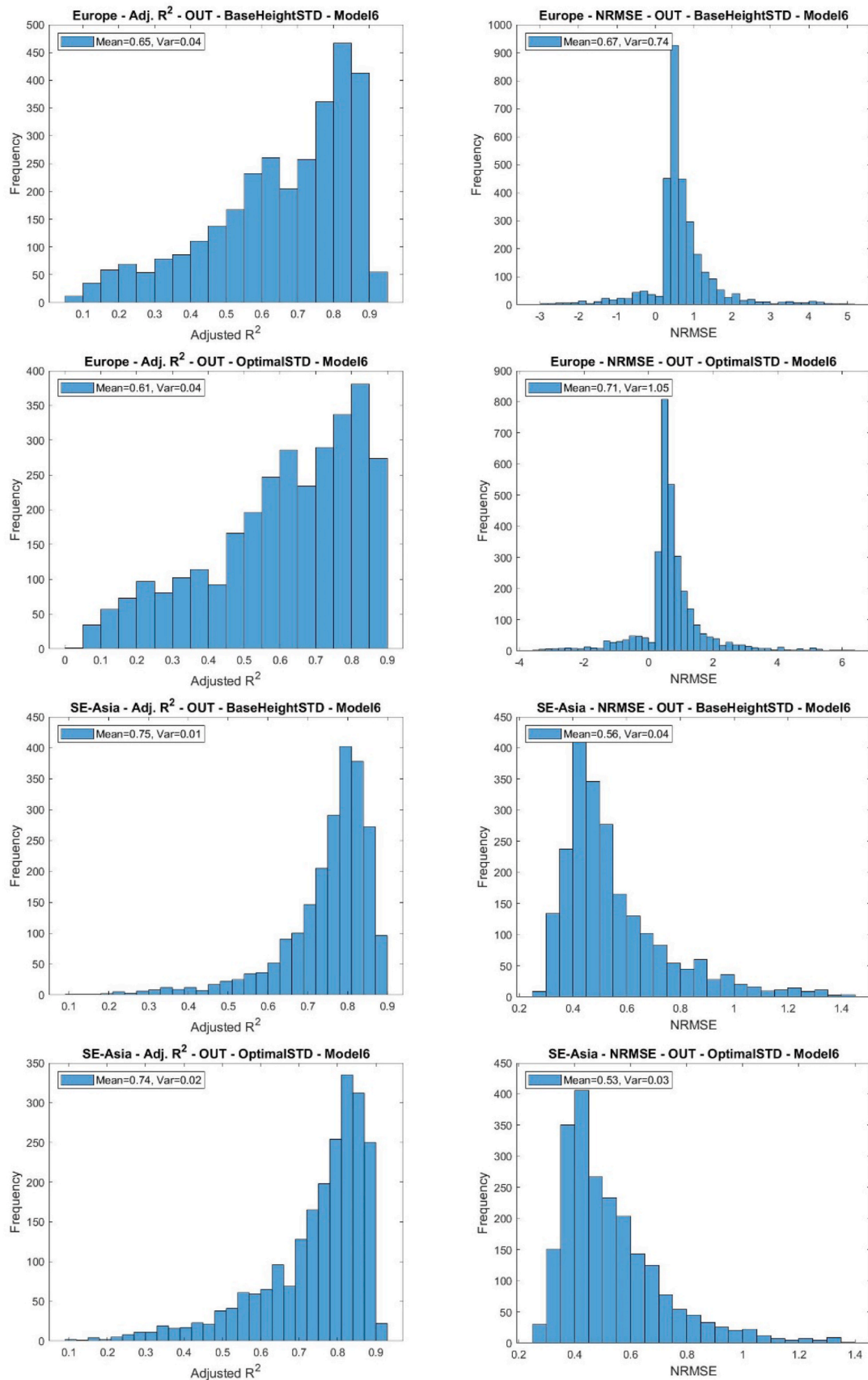
Fig. 5. Forecasting performance and model fit of Model 6 as measured by the out-of-sample (OUT) distribution of NRMSE and adjusted R2 in Europe and South-East Asia.

standards in flood risk models. *BaseProbStd* is also set aside as it assumes that countries monitor the flood probability level and upgrade their standards to keep the flood probability constant, a policy that many developing countries are currently not pursuing. Nevertheless, the comparison of regression estimates for the *NoStd* and *BaseProbStd* case can be found in Table 5 and are available in the CLIMRISK-RIVER model.

Since there are over 16,000 cells, each with its own adjusted R^2 model estimate, Table 1 reports only the average adjusted R^2 values.

From Table 1, it is clear that the model with the most explanatory power is Model 6, which yields the highest average adjusted R^2 across all flood protection standard assumptions. This is to be expected as Model 6 contains more predictors and, unlike the other models, is able to capture the interaction between the climate regressors. Unlike the R^2, the adjusted R^2 penalizes the use of additional explanatory variables and is therefore comparable across different model specifications. It is also important to note that the explanatory power increases by 0.08 on average between Models 3 and 4 across all protection standard assumptions. Model 4 is the first proposed model to contain precipitation as an additional explanatory variable. Precipitation has often been ignored in integrated assessment models where the sole focus is placed on temperature change. See Table 5 in the appendix for the complete regression coefficients of the CLIMRISK-RIVER model for all protection standard assumptions.

As we are evaluating a nested model with 6 functional forms of increasing number of predictors, we will only focus here on comparisons between Model 3 and Model 6. The main reason for this is that Model 3 represents a functional form similar to that of RICE and CLIMRISK models, with quadratic function of temperature change. This makes Model 3 consistent and comparable to other IAMs, unlike Model 1 which ignores climate factors or Models 2, 4 and 5 which include them but either ignore the quadratic terms of temperature/precipitation or the interaction between the two. The model fit to GLOFRIS data is shown in Fig. 3. Two main conclusions can be drawn from these figures. First, Model 6 has a better fit to actual data than Model 3 as is measured by the mean-normalized RMSE and adjusted R^2. The variance of the mean-normalized adjusted R^2 is lower under Model 6. Whereas Model 3 only accounts for GDP and first order temperature change, Model 6 also accounts for precipitation and the squared and interaction terms of temperature and precipitation. Second, Model 6 is able to predict future projected GLOFRIS estimates reasonably well with the majority of predictions not over or underestimating by more than 1.5 times the mean value of the projected GLOFRIS damage.

The spatial distribution of adjusted R^2 and NRMSE in Europe and South-

The spatial distribution of adjusted R^2 and NRMSE is presented for Europe and South-East Asia in Fig. 4 along with their respective histograms in Fig. 5. The two regions were selected for presentation as Europe is expected to experience the lowest amount of flood damage and South-East Asia the highest. South-East Asia is also among the least flood protected regions in the world, whereas the opposite is true of Europe. It is apparent from Fig. 4 that in the northern region in India around the Ganges river, where damage estimates are among the highest in the world, the model forecasts damage reasonably well with NRMSE of around 0.5. The same is true of the North-Eastern part of China in the Yangtze river basin. In Europe, the adjusted R^2 is higher in central and western parts than in north-eastern Europe, in the Baltic region. There is no clear spatial pattern with respect to NRMSE.

From the histogram plots, it is apparent that most adjusted R^2 values are greater than 0.5 and that most NRMSE values are lower than 2. The model fit is good in Europe, with a mean of 0.65 (0.61) and a variance 0.04 for the *BaseHeightStd* (*OptimalStd*). In South-East Asia, the fit is even better with a mean adjusted R^2 of 0.75 (0.74) for the *BaseHeightStd* (*OptimalStd*) and variance of 0.02. The out-of-sample (OUT) explanatory power of *BaseHeightStd* seems slightly higher than that of *OptimalStd* in both regions. This can be explained by the fact that protection standards play an important role in forecasting future flood-related damage,

weakening the climate signal that feeds into CLIMRISK-RIVER.[11]

Having performed various model validity checks, we can now explore the regression results using the regression coefficients from the out-of-sample validation for different flood protection standard assumptions. Table 5 in the appendix illustrates coefficient distributions for each protection standard assumption for Model 6. An important conclusion that can be drawn from these results is that protection standards play an important role in producing the annual expected damage estimates. As the flood protection assumption is changed from *NoStd* towards *OptimalStd*, the climate change signal (temperature and precipitation) weakens, while the GDP signal remains strong but with a smaller effect. Therefore, the key determinant of climate change related flood risk under the economically optimal protection standard is not the climate change but the standard itself and the total economic output. Increased economic output mostly leads to higher river flood damage across all protection standards, with the median independent impact of a $ 1 billion increase in GDP leading to a $0.1–2.4 million increase in EAD across all scenarios (Table 5 column 4). Temperature increase is expected to increase flood damage, but the median effect is zero across all cells for most protection standard assumptions. The effect of precipitation is also in the direction that it leads to more river flood damage for most cells. The median effect of a 1% increase in annual total precipitation on additional flood damage across all cells is around $0.02 million for the *NoStd* and $ 0 million for *OptimalStd*. The mean effect of squared terms varies, but overall indicates that many cells experience increasing damage to temperature and precipitation increase. This property of the damage functions is important as it helps in capturing nonlinear responses of flood damage to higher temperature and precipitation (Nordhaus, 1992). The interaction term is positive on average, indicating that temperature and precipitation reinforce each other's impact on total damage. In other words, wet-hot regions are subject to more severe flooding than dry-hot regions.

3.2. Aggregate flood risk

Next, we look at the development of climate change related flood risk on an aggregate level, firstly on a regional and continental and then on a country level. Fig. 6 shows the evolution of river flood risk on a global scale and in several regions: United States, Europe, Africa, South-East Asia and Latin America. The results do not vary significantly between different RCP scenarios in the first half of the century, but start to diverge in the second for both adaptation assumptions. The reduction in river flood risk is much greater with improved protection standards than with a stricter emission reduction policy, regardless of the RCP scenario or region. This is evident from the spread between the red and blue lines corresponding to *BaseHeightStd* and *OptimalStd*. Under the *BaseHeightStd* on the global scale, the expected river flood damage could reach $3.5 trillion in 2100. The evolution of climate related river flood damage is similar in Europe, with damage reaching $25–30 billion in 2100. South-

---

[11] The GLOFRIS modelling framework uses a global hydrology and water resource model at 5′ x 5′ resolution and downscaled to 30″ x 30″ resolution which simulates fluvial flooding based on a 2D volume river routing model. This flood model shows the best results for Europe and North America, where the meteorological forcing is generally more accurate as a result of availability of station data and reanalysis products (Sutanudjajaet al., 2018). This is in line with the projection accuracy of CLIMRISK-RIVER which shows the highest values of R2 and the lowest RMSE on average in Europe and the US. Furthermore, due to the strong seasonality in forcing and discharge, monsoon-dominated areas are also well simulated. The least accurate results are obtained in African rivers due to groundwater dynamics, snow-dominated areas, and continental eastern Europe, because of overestimations in groundwater recession constants (Sutanudjajaet al., 2018). For readers who are interested in more information about the physical reasoning behind the GLOFRIS flood risk results and strengths and weaknesses we refer to the original GLORIS paper.
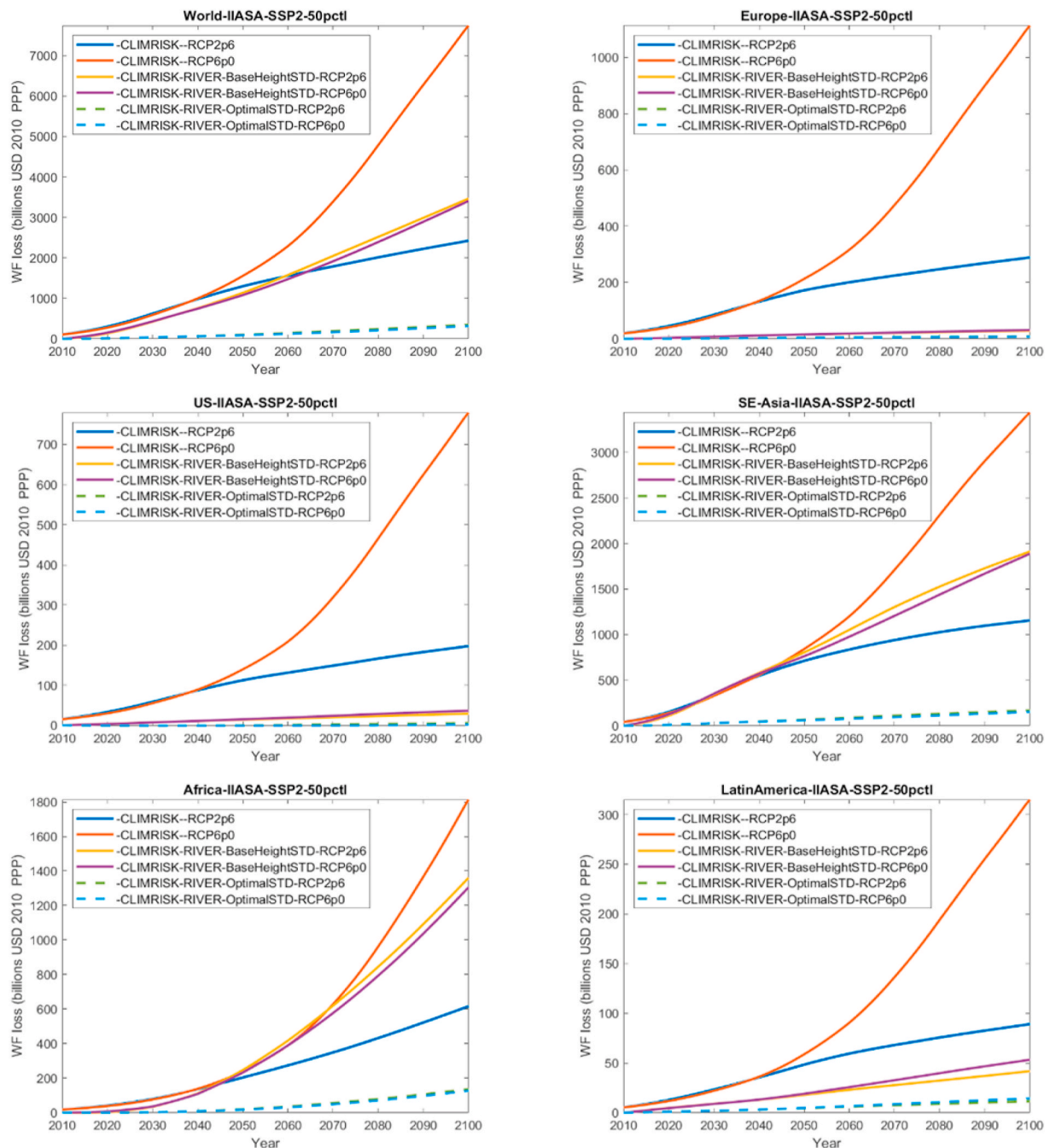
Fig. 6. Annual economic damage in CLIMRISK and ΔEAD in CLIMRISK-RIVER under different protection standards and climate assumptions. Regional inequalities of river flood damage exist and are in some cases comparable in size to previously estimated total climate damage estimates in CLIMRISK model (SE-Asia and Africa).

East Asia and Africa are expected to experience the bulk of the total global damage, $1.5–2.5 trillion and $1.2 trillion respectively in 2100. When optimal adaptation is introduced, the expected damage is reduced drastically on a global scale, to around $ 250 billion in 2100. However, the damage reduction is relatively lower in Europe (around $5–10 billion, a 66% reduction) when compared to South-East Asia (around $ 200 billion, 90% reduction) and Africa (around $140 billion, a 90% reduction). The main reason for this drastic regional difference is the fact that the protection standards already in place in the developed world are close to (or at) the optimal level of protection standards. Introducing the optimal level of protection standards ensures that the river flood damage due to climate change does not exceed 30% and 10%

of the business-as-usual potential damage in Europe and South-East Asia/Africa respectively.

To put climate change-related river flood risk into the perspective of total damage from climate change, we compare the results of our model with the damage in CLIMRISK.[12] Fig. 6 presents the evolution of CLIMRISK and CLIMRISK-RIVER for different regions in the world[13]. On a global scale (top-left), the ΔEAD under the *BaseHeightStd* assumption is

---

[12] The plotted CLIMRISK values do not account for CLIMRISK-RIVER estimates (i.e. before CLIMRISK-RIVER integration).

[13] More results for other protection standard assumptions can be found in Appendix C Fig. 18.
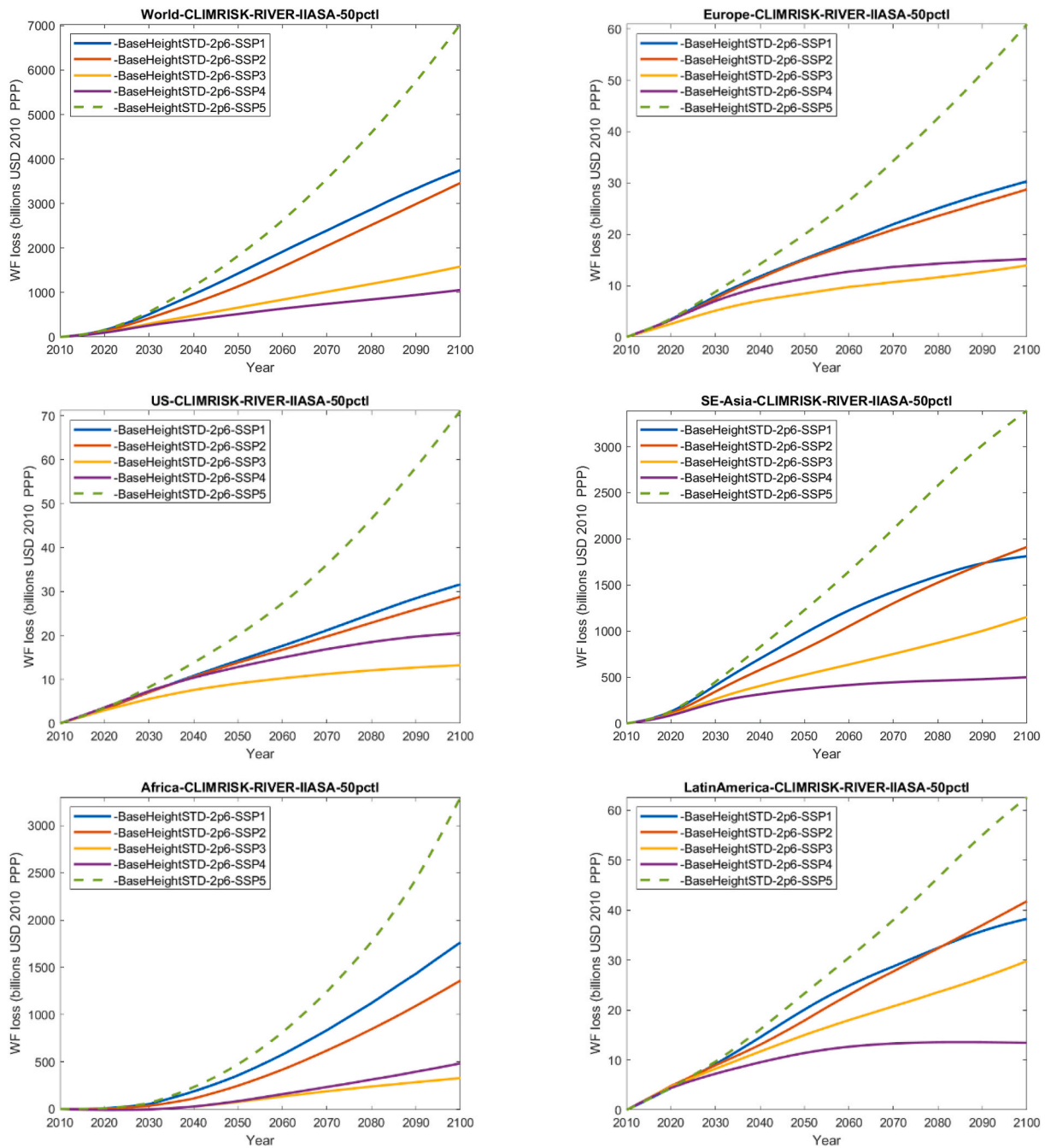
Fig. 7. ΔEAD in CLIMRISK-RIVER under different socio-economic projections (SSP scenarios). The wide uncertainty range in flood damage projections is captured, highlighting the importance of socioeconomic scenario assumption used.

equivalent to 50% of the CLIMRISK model damage projections for the RCP 2.6 - SSP2. South-East Asia and Africa are expected to experience a large increase in flood risk, because adequate flood protection standards are lacking or non-existent in many areas. The opposite is true in Europe and the United States, where CLIMRISK-RIVER projects river flood damage of much lower magnitude than the CLIMRISK damage projections. On an aggregate level, the river flood damage under the *BaseHeightStd* assumption presents a relatively lesser threat to Europe and the United States than to the less developed world of South-East Asia and Africa. Another important conclusion that can be drawn from Fig. 6 pertains to the relative impact of climate mitigation under the two models. Namely, the CLIMRISK model is more sensitive to climate change mitigation than CLIMRISK-RIVER as indicated by the relative

difference in damage estimates under the RCP 2.6 and RCP 6.0 climate scenarios.

Socio-economic development plays an important role in future flood risk as it determines the number of exposed assets. Fig. 7 illustrates flood risk estimates under different SSP scenarios and the RCP 2.6 climate scenario. In all regions, the SSP5 scenario of fossil fuel development would universally lead to the highest expected river flood damages. The SSP3 and SSP4 scenarios, both involving a relatively high level of climate adaptation compared to that of other SSPs, would lead to the lowest expected river flood damages in most regions.

3.2.1. Country-level CLIMRISK-RIVER

In this section, we present the CLIMRISK-RIVER damage estimates on
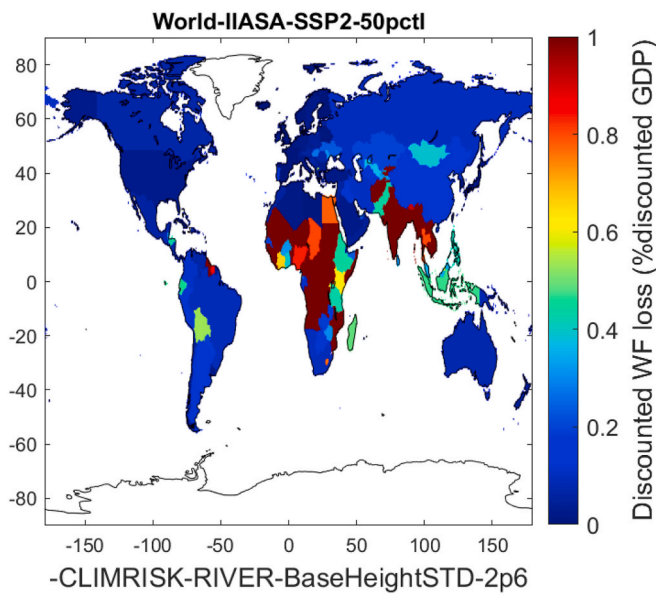
Fig. 8. World map of discounted total ΔEAD expressed as a percentage loss of discounted GDP for the period 2010–2100. The fill color represents the severity of damage under the BaseHeightStd flood protection assumption and RCP 2.6 climate scenario.

Table 2

Top 10 most endangered countries in the world[a] and in Europe[b] in the twenty first century, as measured by the discounted total ΔEAD (billion $USD, 2010) due to climate change (columns 2–5). The presented discounted damage estimates refer to the sum of $0.5° \times 0.5°$ cells belonging to a specific country for SSP2 scenario using IIASA projections (see Appendix A).

World ΔEAD	Climate Scenario RCP 2.6		Climate Scenario RCP 6.0	
Country	*BaseHeightStd*	*OptimalStd*	*BaseHeightStd*	*OptimalStd*
India	8219	789	7776	757
DRC	2238	13	2160	13
China	1950	138	1990	144
Cambodia	1218	144	1199	141
Bangladesh	1084	136	1043	130
Vietnam	564	25	572	25
Indonesia	540	521	499	79
Myanmar	401	9	380	10
Thailand	384	23	395	23
Nigeria	361	15	334	15
Europe ΔEAD	Climate Scenario RCP 2.6		Climate Scenario RCP 6.0	
Country	*BaseHeightStd*	*OptimalStd*	*BaseHeightStd*	*OptimalStd*
Russia	113.36	21.22	109.78	19.99
Ukraine	48.85	4.71	46.92	4.71
Germany	26.67	11.31	29.45	11.73
Hungary	26.50	1.55	27.56	1.70
Portugal	17.61	16.15	17.79	16.30
Italy	13.96	6.18	13.83	6.13
Poland	11.67	2.31	12.08	2.50
Austria	11.45	2.75	12.11	3.10
France	11.06	7.14	11.68	7.18
Turkey	10.11	2.75	10.54	2.95

[a] Rounded to the nearest integer.
[b] Rounded to two significant digits.

a country level. The damage estimates are presented in terms of discounted ΔEAD relative to the discounted GDP for the period 2010–2100. Fig. 8 below presents a world map of country-level damage estimates for the BaseHeightStd adaptation scenario.

Table 2 shows the top 10 countries in the world [14] and in Europe [15] in terms of highest discounted total ΔEAD in the CLIMRISK-RIVER model. Eight of the ten global highest are in South-East Asia and two in Africa, specifically the Democratic Republic of Congo (DR Congo) and Egypt. The discounted climate change related river flood damage in the top 10 most affected countries in the world is around $16 trillion, which could be brought down to about $300 billion by implementing the optimal level of flood protection standards under the RCP 2.6 scenario. In Europe, damages are much lower with a combined total of around $105 billion dollars of discounted total ΔEAD in the top 10 countries under the RCP 2.6 scenario and with $110 billion under RCP 6.0. This damage could be reduced by adopting an optimal flood protection policy, bringing them down to around $25 billion under both RCP 2.6 and RCP 6.0. To conclude, European countries stand to gain relatively less from additional adaptation than the most affected countries in the world because the adaptation standards already in place in many European countries are high. Please note that it is possible for the damage under RCP 2.6 to be higher than under RCP 6.0 scenario due to varying natural factors accounted for in GLOFRIS (precipitation, temperature, evaporation etc.). Some regions could become wetter or drier with increasing temperature or could switch between wet and dry periods throughout the twenty-first century depending on varying natural factors. This effect could ultimately determine the total damage due to river flooding.

3.3. Local flood risk

In this section, we analyze the local impacts of river flooding due to climate change. This involves the estimation of the discounted value of river flood damage due to climate change at the grid cell-level along with city-level estimates. Fig. 9 illustrates the effect that flood adaptation standards have on the expected flood damage due to climate change. The selected scenario combination in this figure is RCP 6.0 - SSP2 and the damages are expressed as a fraction of discounted GDP. In Europe, the area around the Rhine river basin would benefit from additional flood adaptation. There are also clear benefits to river flood adaptation in Eastern Europe, around the northern coast of the Black Sea (Ukraine). The greatest benefits from optimal protection standards can be observed in South-East Asia and Africa. The northern region of India is expected to experience serious flooding due to climate-change along the Ganges river basin under the current level protection. In China, the Yangtze river is also expected to cause significant damage to the built environment. In Africa, the Nile river poses a flood threat under the baseline protection standards. Central Africa also stands to benefit greatly from river flood adaptation along the Congo river basin as most of these areas currently have low (or no) river flood protection standards.

In the following subsection, we focus on cells most severely affected by future flood risk and identify cities that fall within their boundaries.

3.3.1. City-level CLIMRISK-RIVER

River flooding represents a serious threat to the built environment, especially in areas wherein flood protection standards are lacking and many assets are exposed. Most cities are built around rivers or other available bodies of water, which makes them vulnerable to flooding, and this is particularly the case in overpopulated cities that are less developed and lack flood protection. Although CLIMRISK-RIVER does not produce city-level estimates, we identify in Table 3 the cities in the world residing in cells that are expected to experience the most discounted total ΔEAD between 2010 and 2100. This is not a perfect measure of city-level flood risk, but helps us identify the cities located in most flood risk prone areas. The first half of the table consists of city-cells that are expected to experience the most discounted damage in

---

[14] Rounded to the nearest integer.
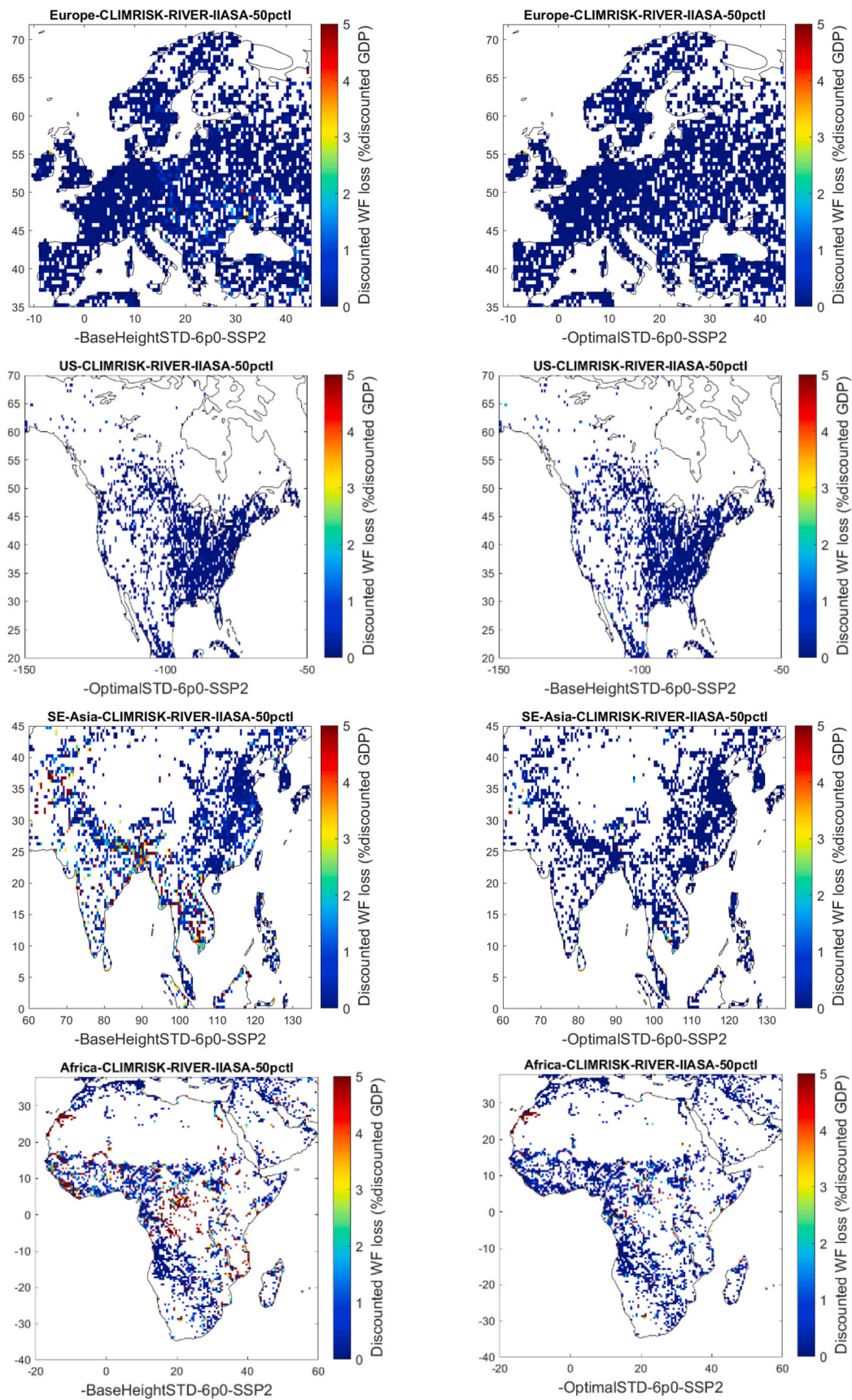[15] Rounded to 2 significant digits.

Fig. 9. Local CLIMRISK-RIVER: Discounted annual expected damage on a grid cell level for BaseHeightSTD (left panel) and OptimalSTD (right panel) flood protection standards for different regions.

Table 3

Top 10 most endangered city-cells in the world[a] and in Europe[b] in the twenty-first century, as measured by the discounted total ΔEAD (billions $USD, 2010) due to climate change (columns 3–6).

World ΔEAD City-cell		Climate Scenario RCP 2.6		Climate Scenario RCP 6.0	
		BaseHeightStd	*OptimalStd*	*BaseHeightStd*	*OptimalStd*
Mumbai	IND	732	591	703	569
Kisangani	COD	588	3	562	3
Kakinada	IND	515	3	482	3
Kolkata/Haora	IND	499	3	494	3
Rajahamundry	IND	287	2	269	2
Dongguan	CHN	278	74	275	72
Mbuji-Mayi	COD	209	1	197	1
Varanasi	IND	190	2	161	2
Phnom-Penh	KH	168	1	166	1
Bhubaneshwar	IND	141	1	145	1
Europe ΔEAD City-cell		Climate Scenario RCP 2.6		Climate Scenario RCP 6.0	
		BaseHeightStd	*OptimalStd*	*BaseHeightStd*	*OptimalStd*
Gyor	HU	18.03	0.07	18.88	0.08
Porto	PT	15.57	15.03	15.81	15.26
Kiev	UKR	9.39	1.22	8.93	1.19
Frankfurt	DE	7.10	1.27	8.13	1.43
Cologne	DE	5.16	1.27	5.97	1.38
Zurich	CH	4.53	4.37	4.52	4.33
Kharkiv	UKR	4.22	0.18	4.11	0.18
Vienna	AU	3.96	0.91	4.20	1.08
Chisinau	UKR	3.87	3.87	4.23	4.23
Lysychansk	UKR	3.82	0.16	3.74	0.16

[a] Rounded to nearest integer.
[b] Rounded to two significant digits.
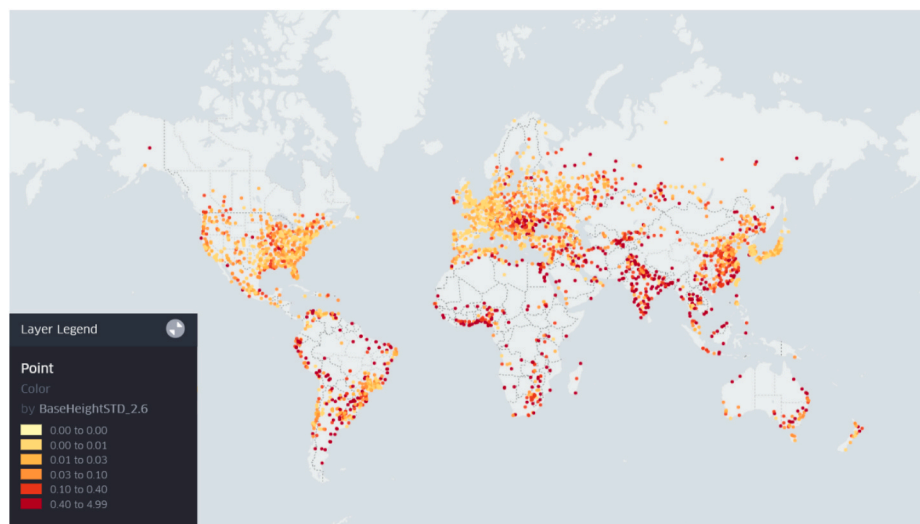
Fig. 10. World cities located in low-risk cells with discounted ΔEAD of less than 5% discounted GDP. The presented results correspond to the scenario combining RCP 2.6, SSP2 and BaseHeightStd assumptions.:

the world. Here, eight of the ten city-cells belong to India and two in DR Congo. The reasons for this include relatively low flood protection standards as witnessed by the benefits of flood adaptation under the *OptimalStd* assumption, a high potential for flooding around the Ganges river basin, and an abundance of exposed assets.

The top 10 European city-cells are expected to experience relatively less damage, with a total discounted Δ*EAD* of around $ 80.45 billion under RCP 2.6 and the *BaseHeightStd* assumption. Still, there are benefits from *OptimalStd* that result in around $31.55 billion discounted Δ*EAD*.[16]

Under RCP 6.0 the situation is similar, with *BaseHeightStd* leading to $33 billion and *OptimalStd* to $5.6 billion additional damage. The bulk of this damage would be experienced around the Danube river basin in Eastern Europe, as was also evident from Fig. 9.

We are interested in the difference in expected flood risk among city-cells and express the damage projections as a fraction of GDP[17]. Using this method, we define the following four arbitrary risk categories:

1. *Low-risk city-cells*: Discounted Δ*EAD* of less than 5% discounted GDP;
2. *Medium-risk city-cells*: Discounted Δ*EAD* between 5% and 25% of discounted GDP.

---

[16] Please note that this estimate is heavily influenced by the fact that the city of Porto is facing a high flood risk under both BaseHeightSTD and OptimalSTD, meaning that there is insufficient space for flood adaptation improvement.

[17] Discounted Δ*EAD* and GDP are both for the period 2010–2100 at 3%.

Fig. 11. *World cities located in medium-risk cells with discounted ΔEAD exceeding 5% but not 25% of discounted GDP. The presented results correspond to the scenario combining RCP 2.6, SSP2 and BaseHeightStd assumptions.*

3. *High-risk city-cells*: Discounted Δ*EAD* between 25% and 100% of discounted GDP.

4. *Very-high-risk city-cells*: Discounted Δ*EAD* of more than 100% discounted GDP.

Fig. 10 presents low-risk city-cells, in particular those that could experience less than 5% GDP in discounted total Δ*EAD*. Most cities globally fall within this category.

The medium-risk category is presented in Fig. 11. Fewer city-cells in the developed world belong in this category, and most cells can be found in Latin America, Africa and South-East Asia.

The high-risk category is presented in Fig. 12 and isolates city-cells almost exclusively in Africa, Latin America and South-East Asia. Gyor in Hungary is the cell in Europe belonging to a high-risk category.

Fig. 13 presents city-cells which belong to a very high-risk group of cells. As expected, the most affected cells could be found exclusively in Central Africa (Dr. Kongo) and in Latin America in areas with low river flood protection standards.

4. Discussion

The CLIMRISK-RIVER model was developed using the spatially-explicit damage estimates and flood protection standards from the GLOFRIS and FLOPROS models. Several model specifications were tested and the best performing statistical model - Model 6 - was selected as the CLIMRISK-RIVER model. The process of selecting the most suitable model among different candidates was based on the measure of statistical fit to the GLOFRIS model data. However, the proposed model candidates were chosen with general climate and economic predictors in mind to remain intuitive and easy to use, thereby avoiding the issue of overfitting and going beyond simple emulation.

Several validation methods were applied to the newly estimated model. We first looked at the spatial and frequency distributions of the adjusted R^2 statistics for all cells. The model performs reasonably well on a global scale, the mean adjusted R^2 of the model being 0.69 and 0.66 for the *BaseHeightStd* and *OptimalStd* assumptions respectively. We also measured the model forecasting performance through within-sample and out-of-sample NRMSE. With an average out-of-sample 5-fold NRMSE value of 0.69 and a variance of 0.17 across all cells, we can
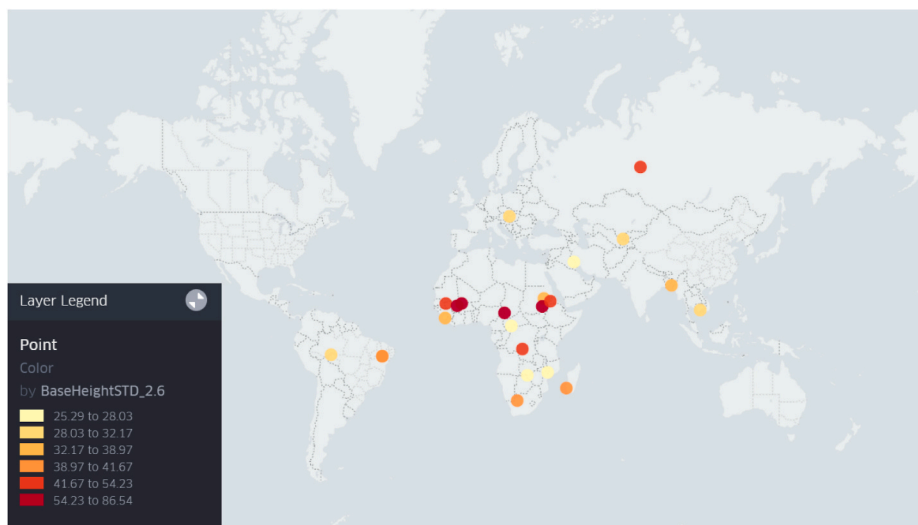

Fig. 12. *World cities located in high-risk cells with discounted ΔEAD exceeding 25% but not 100% of discounted GDP due to river flooding. The presented results correspond to the scenario combining RCP 2.6, SSP2 and BaseHeightStd assumptions.*
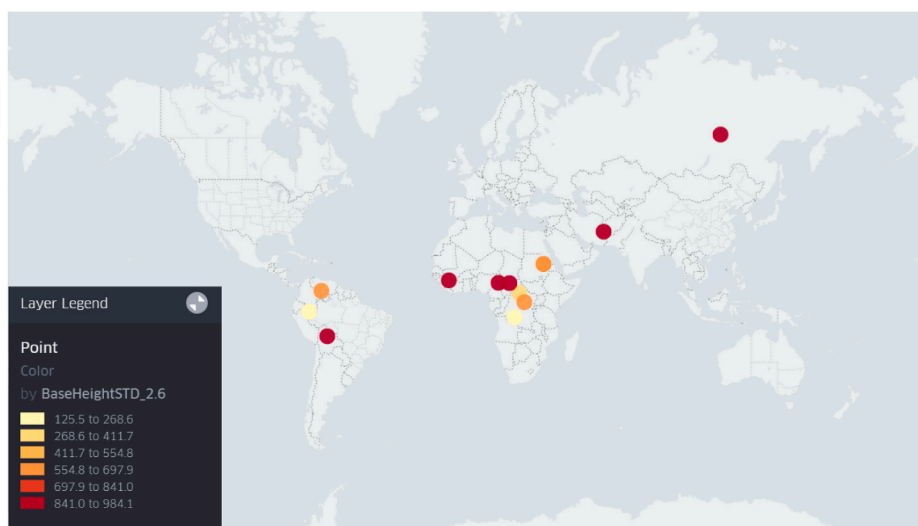
Fig. 13. *World cities located in very high-risk cells with discounted ΔEAD exceeding 100% discounted GDP. Most of the cells are located in Central Africa. The presented results correspond to the scenario combining RCP 2.6, SSP2 and BaseHeightStd assumptions.*

Table 4
RICE damage function coefficients as in (Nordhaus, 2017).

Region	α_r	β_r
Africa	0.3410	0.1983
China	0.0785	0.1259
EU	0	0.1591
Eurasia	0	0.1305
India	0.4385	0.1689
Japan	0	0.1617
Latin America	0.0609	0.1345
Middle - East	0.2780	0.1586
Other Asia	0.1755	0.1734
Other High Income	0	0.1564
Russia	0	0.1151
US	0	0.1414

confirm that the model performs reasonably well on previously unseen data. This grants confidence to our approach.

To gain a better understanding of the magnitude of CLIMRISK-RIVER damage estimates within the total climate change-related damage, the results are plotted against total CLIMRISK damage estimates. On a global scale, under the *BaseHeightStd* flood protection scenario, the climate-related damage due to river flooding could exceed previously estimated total climate damage in CLIMRISK[18] of $2 trillion in year 2100. However, when the economically optimal flood protection policy is introduced, the estimated damage drops down to just around $ 250 billion, an estimated ten-fold decrease in global river flood damage at the end of the century. These results highlight the importance of accounting for adaptation in estimating the damage functions for IAMs. However, the divergent estimates under the different adaptation assumptions also reveal that adaptation policies introduce an important uncertainty in forecasting future flood risk.

There are also some limitations of the model which require attention. Firstly, we are focusing on emulation of a complex river flood risk model and approximate the underlying physical and socio-economic processes to gain on both model and computational simplicity, which results in structural model uncertainties. For instance, flood damage development depends on the severity of flooding, which is approximated with annual resolution climatic variables used in this study to emulate damage. Changes in weather extremes are not accounted for in the current work

for the sake of ease of model implementation within the broader CLIMRISK model. Moreover, it should be realized that the flood damage functions are based on GLOFRIS results forced with GCM simulations rather than recorded climatic data in which annual trends may be less clearly aligned with occurrence of extremes. Climate-economy IAMs inevitably require reduced form damage functions, like we estimated for CLIMRISK-RIVER, and despite the limitations we have confidence in our approach given the overall good forecast performance of our model.

There are possibilities for improving the presented model in future work. One point of improvement could be the function estimation method. For example, different model specifications could be used, including (non-)linear interpolation or even less orthodox non-parametric methods (splines, bootstrapping, etc.). However, adding more degrees of freedom to the model should be done with care as this could lead to overfitting to the GLOFRIS estimates and complex damage functions, both of which CLIMRISK-RIVER attempts to avoid.

5. Conclusion

In this paper we presented CLIMRISK-RIVER, a climate change-related river flood damage assessment model that is integrated in a spatially explicit climate-economy IAM called CLIMRISK. The newly developed model operates on a local, spatially explicit scale and can project future climate change related river flood damage estimates for various socioeconomic, climate, and flood adaptation scenarios. The main idea behind the development of such a model was the need for generic damage functions that can be used with any climate and socioeconomic scenarios. This means that the user will be able to select any climate and socioeconomic scenario combination, including future to be developed versions of scenario projections, as long as they have local temperature, precipitation and GDP estimates to feed into the model.

Two traits of the CLIMRISK-RIVER model are unique in the existing literature on climate-economy IAMs. First, its local nature allows the user to explore river flood damage projections for $0.5° \times 0.5°$ cells anywhere in the world. This is much more detailed than most climate-economy IAMs that apply global damage functions or estimate the economic impacts of climate change for several world regions.

Second, its inclusion of current and future adaptation scenarios that account for local river flood protection standards in generating the damage estimates is unique in existing literature of IAMs. Few existing climate-economy IAMs explicitly account for adaptation using policy relevant scenarios.

_____
[18] RCP 2.6 – SSP2, Fig. 6.

Four main conclusions can be drawn from our analysis. First, our validation exercise shows that our reduced form flood damage functions estimated at the grid cell level perform reasonably well in capturing estimates produced by the more detailed flood damage model GLOFRIS.

Second, while IAMs have relied on temperature as a proxy for climate change in generating economic impacts, we show that precipitation is a relevant additional explanatory variable in projecting changes in river flood damages.

Third, our aggregated results for several large regions show that the additional flood damages from climate change are non-negligible compared to the total economic impacts estimated by CLIMRISK, although this depends on the flood adaptation scenario.

Finally, the spatially heterogeneous results that we presented for countries and cities reveal the importance of introducing local-scale estimates like GLOFRIS into a more local IAM like CLIMRISK. These findings demonstrate the advantages of the local nature of our model, which allows the user to observe the spatial distribution of river flood damage that are otherwise lost through aggregation.

Funding

Declaration of competing interest

Acknowledgements

Appendix H. Supplementary data

Supplementary data related to this article can be found at https://doi.org/10.1016/j.envsoft.2020.104784.

Appendix A. CLIMRISK model

The flood risk model CLIMRISK-RIVER (CLIMRISK-RIVER) developed in this paper is introduced into the CLIMRISK model that operates on a local $0.5° \times 0.5°$ or larger scale (Estrada and Botzen, 2018). CLIMRISK is a global model that assesses the dynamic economic impacts of climate change at the local scale (0.5 x 0.5°) for various socioeconomic and climate change projections. This is done by combining local GDP exposure information (Grübler et al., 2007) with climate projections obtained using the MAGICC climate model and scaling patterns from the climate models included in the CMIP5 (Lynch et al., 2017), (Kravitz et al., 2017). Regional impact functions are taken from the RICE model and encompass a broad range of economic sectors (Nordhaus, 2017), (Estrada et al., 2017). The result is a global, dynamic, integrated assessment model that projects climate damages on a local, regional and global scale. The CLIMRISK model is composed of the following interlinked components:

1. **Hazard:** Climate change projections
2. **Exposure:** Economic projections
3. **Vulnerability:** Impact functions

These modules build upon and integrate well-established models, datasets, techniques and procedures that have been previously evaluated and published, as will be explained next.

1 Hazard: Climate projections

CLIMRISK combines probabilistically generated global temperatures with the regional precipitation and temperature scaling patterns from 41 general circulation models (GCM) in the CMIP5 database (Lynch et al., 2017), (Kravitz et al., 2017). For the global and regional probabilistic estimates of climate projections, CLIMRISK uses the MAGICC version 6 software. MAGICC represents a reduced-complexity model of climate change and is widely used in the research community to project future climate impacts (Meinshausen et al., 2011), (Meinshausen et al., 2011),(van Vuuren and Carter, 2014), (Barker, 2007). It also relies on the technique of pattern scaling to produce local estimates of temperature and precipitation change. The MAGICC projections used in CLIMRISK are the difference in annual mean temperatures (in degrees Celsius) and precipitation (in %) with respect to 1900. The spatial patterns of different GCMs are randomly selected using a uniform distribution (Weigel et al., 2010), (Knutti, 2010). CLIMRISK imposes a triangular probability distribution for the climate sensitivity parameter. This particular distribution is centered around a lower limit of 1.5 °C, an upper limit of 4.5 °C and a mean value of 3 °C for climate sensitivity (Stocker et al., 2013). The triangular distribution of temperature realizations is a measure of climate sensitivity in the CLIMRISK model. By representing it using a probability distribution the IAM is able to produce temperature rise estimates that encompass the likely ranges of climate change. As precipitation realizations directly depend on temperature realizations in MAGICC, the triangular distribution covers both climate variables in the model. For the purposes of this paper, only the median (50th percentile) realizations are used for all scenario combinations.

2 Exposure: Economic projections

Scenarios of GDP determine the economic exposure to the climate change hazard (A.1), which is an important input in the damage functions for the climate impacts calculation (A.3.). The economic projection data used in CLIMRISK and CLIMRISK-RIVER relies on the GDP and population

projections of the SSP Public Database Version 1.1 .[19] In order to construct spatially explicit information, CLIMRISK combines the Shared Socio-Economic Pathways (SSP) and Special Report on Emissions Scenarios (SRES) projections available through the GGI Scenario Database Version 2.0.1 (http://www.iiasa.ac.at/Research/GGI/DB/) (Rao et al., 2008), (Riahi et al., 2017), (Grübler et al., 2007). These databases are commonly used in climate impact studies and gather a variety of scenarios about GDP and population that have been produced by different modeling groups. This procedure of combining SSP and SRES data can be done due to the fact that certain SRES and SSP scenarios are consistent with each other (Riahi et al., 2017). For example, A1 or B1 and the SSP1, SSP5 narratives represent a similar pattern of socio-economic development, the A2 scenario would make SSP3 and SSP4 scenarios plausible, while the B2 SRES is consistent with SSP2 (van Vuuren and Carter, 2014). The pattern scaling method used in CLIMRISK is similar to that in other general circulation models (Kravitz et al., 2017), (Tebaldi and Arblaster, 2014). The grid-cell i's pattern spatial pattern, labelled as $P_{i,t}$, represents the proportion of GDP or population in cell i within region r to the regional total across all cells I:

$$P_{i,t} = \frac{Y_{i,t}^{SRES}}{\sum_{t=1}^{I} Y_{i,t}^{SRES}} \tag{6}$$

where cell i belongs to a particular region $i \in r$, $Y_{i,r,t}^r$ is derived from SRES and for every SRES storyline. These patterns are not assumed to be constant over time and are updated every ten-years period. The regional total of the particular SSP scenario can then be scaled by the SRES consistent regional $P_{i,r,t}$ pattern to obtain i's grid-cell level estimate:

$$Y_{i,t}^{SSP} = P_{i,t} * Y_{r,t}^{SSP} \tag{7}$$

By construction, the downscaled scenario projections match exactly the quantifications of the SSP narratives, produced by different modeling groups, at the aggregated 13 world regions and the global totals. CLIMRISK attempts to account for socioeconomic uncertainty by including all the SSP narratives (SSP1, SSP2, SSP3, SSP4, SSP5). In addition, uncertainty in GDP quantification is tackled through the use of economic data provided by three different modelling groups (OECD Env-Growth, IIASA, PIK) (Crespo Cuaresma, 2017),(Dellink et al., 2017),(Leimbach et al., 2017). The IIASA scenarios were selected for the use in CLIMRISK-RIVER because they correspond to the socio-economic projections used in the GLOFRIS model, making the model validation easier. However, using any of the above-mentioned sources is possible when generating river flood damage projections.

3 Vulnerability: impact functions

CLIMRISK relies on the regional damage functions improved estimates of the RICE model (Nordhaus, 2017). These regional damage functions encompass a broad range of economic impacts. Following the RICE model, the impact functions take into account the losses suffered by major economic sectors such as agriculture, but also the cost of sea-level rise, adverse impacts on health, non-market damages and catastrophic damages (Nordhaus, 2014). The damage function in RICE is as follows:

$$D_{r,t}^{RICE} = \alpha_r T_t + \beta_r T_t^2 \tag{8}$$

where α_r and β_r represent the regional temperature coefficients that measure the impact of global mean annual temperature increase on climate related regional economic damage, $D_{r,t}^{RICE}$, measured in billions of dollars (2015 PPP). Table 4 presents the CLIMRISK/RICE regions along with their respective damage coefficients, based on (Nordhaus, 2017):

The damage function defined above lets us derive the RICE regional climate impacts:

$$I_{r,t}^{RICE} = Y_{r,t} D_{r,t}^{RICE} \tag{9}$$

where $Y_{r,t}$ is the annual regional GDP in region r, at time t. When using pattern down-scaled inputs as defined in A.2, the regional damage function can be converted into a local:

$$D_{i,t}^{CLIMRISK} = \alpha_r T_{i,t} + \beta_r T_{i,t}^2 \tag{10}$$

where, as previously defined, α_r and β_r represent the regional temperature coefficients that measure the impact of local mean annual temperature increase $T_{i,t}$ on climate related local economic damage $D_{i,t}^{CLIMRISK}$ in cell i. The total economic impact of climate change in year t in cell i is therefore:

$$I_{i,t} = Y_{i,t} D_{i,t}^{CLIMRISK} S_{r,t}^{RICE} \tag{11}$$

where $Y_{i,t}$ represents the projected output for cell in year t as defined in equation (7) and $S_{r,t}$ represents the scaling factor that ensures that projected damages are exactly the same regardless of whether the regional damage functions are driven by global or grid cell temperatures.

The scaling factor $S_{r,t}$ is defined as:

$$S_{r,t}^{RICE} = \frac{I_{r,t}^{RICE}}{\sum_{i}^{I} I_{i,t}} \tag{12}$$

where $I_{r,t}^{RICE}$ represents the RICE regional impacts and cell i belongs to particular region $i \in r$. Consistent with the RICE model that assumes the same damage function can be applied across areas within a region, across SSP scenarios, and over time, we apply the same RICE damage function to grid cells within a region. This assumption may be seen as restrictive, which is why CLIMRISK-RIVER introduces damage functions for river flood risk that

---

[19] https://tntcat.iiasa.ac.at/SspDb.

vary between grid cells (see Section 2).

In addition to the local impacts based on the RICE damage functions, CLIMRISK also introduces urban damages into the model. Given that the RICE model relies on regional mean surface air temperatures, it is not possible to account for the effect of urbanization on local temperatures in cities using the RICE model, an effect commonly known as urban heat island (UHI). However, the local nature of CLIMRISK makes the modeling of UHI possible. Namely, urban areas (>1 million inhabitants) are likely to experience higher damage due to climate change than non-urban areas as cities account for about 80% of global GDP and about 50% of global population (Re, 2004), (Dobbs et al., 2011). In addition, urban areas are expected to experience higher local temperatures due to the urbanization process. For example, the replacement of natural surfaces with structures of higher thermal capacity (concrete, asphalt etc.) leads to local climate change effects (Estrada et al., 2017). Since the grid cell scale is still likely to cover an area larger than a particular urban city, the total output in an urban cell is divided between the non-urban (20%) and urban (80%) part of the cell. The damage function for the non-urban part of a particular urban cell *i* follows a recently used damage function for urban areas in an IAM for cities (Estrada et al., 2017):

$$D_{i,t}^{T,U} = 0.9 \left(\frac{T_{i,t} + U_{i,t}}{2.5} \right)^2 \tag{13}$$

where $T_{i,t}$ and $U_{i,t}$ represent changes in annual temperature in cell *i* due to global and local climate change, respectively. The combined damage from the non-urban and urban part of the urban cell represents the total expected damage for cell *i* in a given year *t*.

The local temperature increase $U_{i,t}$ in equation (13) is commonly estimated in the following way:

$$U_{i,t} = aPop_{i,t} \tag{14}$$

where $Pop_{i,t}$ represents the urban population of cell *i* at time *t* and parameters *a* and *b* are commonly used in literature for estimating the urban temperature increase due to urbanization (Oke, 1973), (Karl et al., 1988), (Mills, 2014).

Appendix B. Regressions

The coefficients of regressions for all cells in Model 6 are presented in Figure 14, 15, 16 and 17, for various protection standard assumptions. In Table 5, the distribution of different coefficients is presented for Model 6, the chosen CLIMRISK-RIVER model. For presentation purposes, the coefficients in this table are converted to yield damages in millions of $USD instead of billions (as presented in the paper). From the figures, we can observe that the effect of an increase in economic output (GDP) leads to increased exposure and higher river flood damages. The effect is the strongest with no existing flood protection standards (median $2.3 million) and drops significantly when optimal standards are employed (median $0.1 million) for every $1 billion increase in GDP. We can also observe that the effect of precipitation is stronger with no existing standards (median $1.1 million) than in other cases (median $0.1million) for a 1% point increase in precipitation. The effect of temperature remains ambiguous, with median value of $0 across all flood protection assumptions.
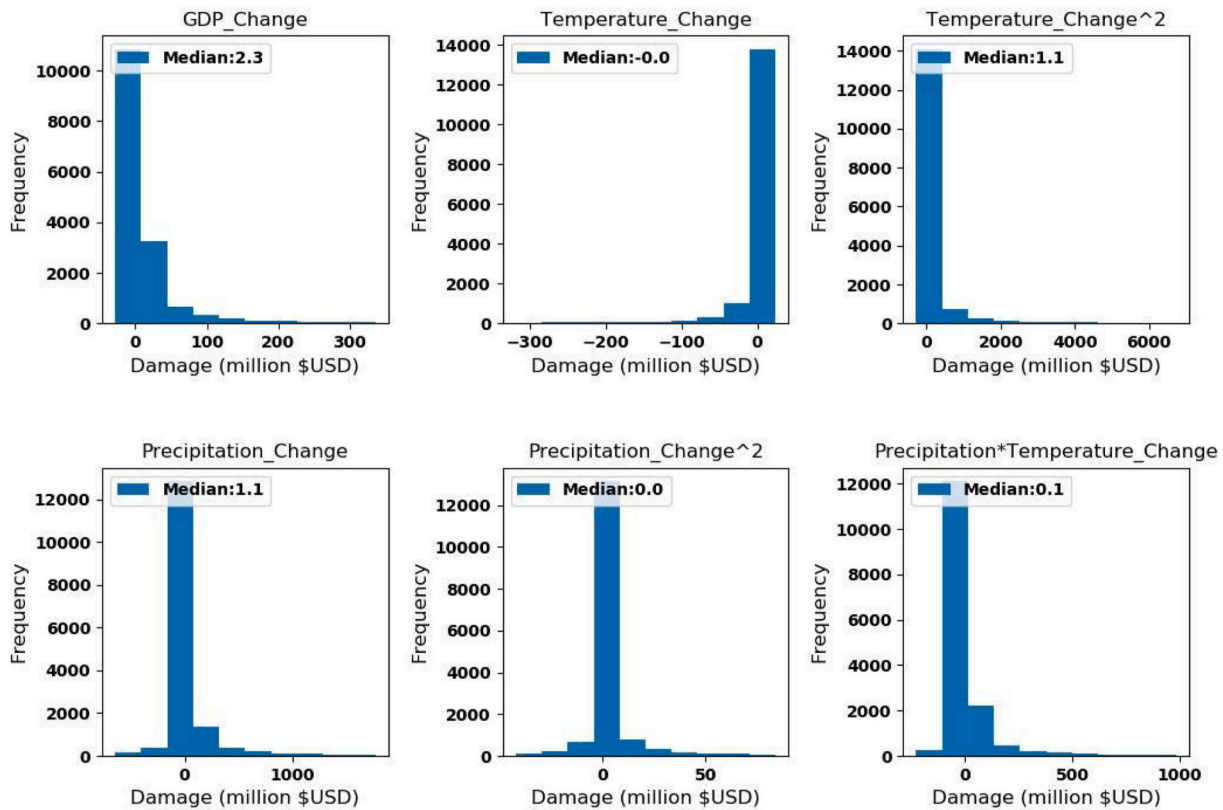

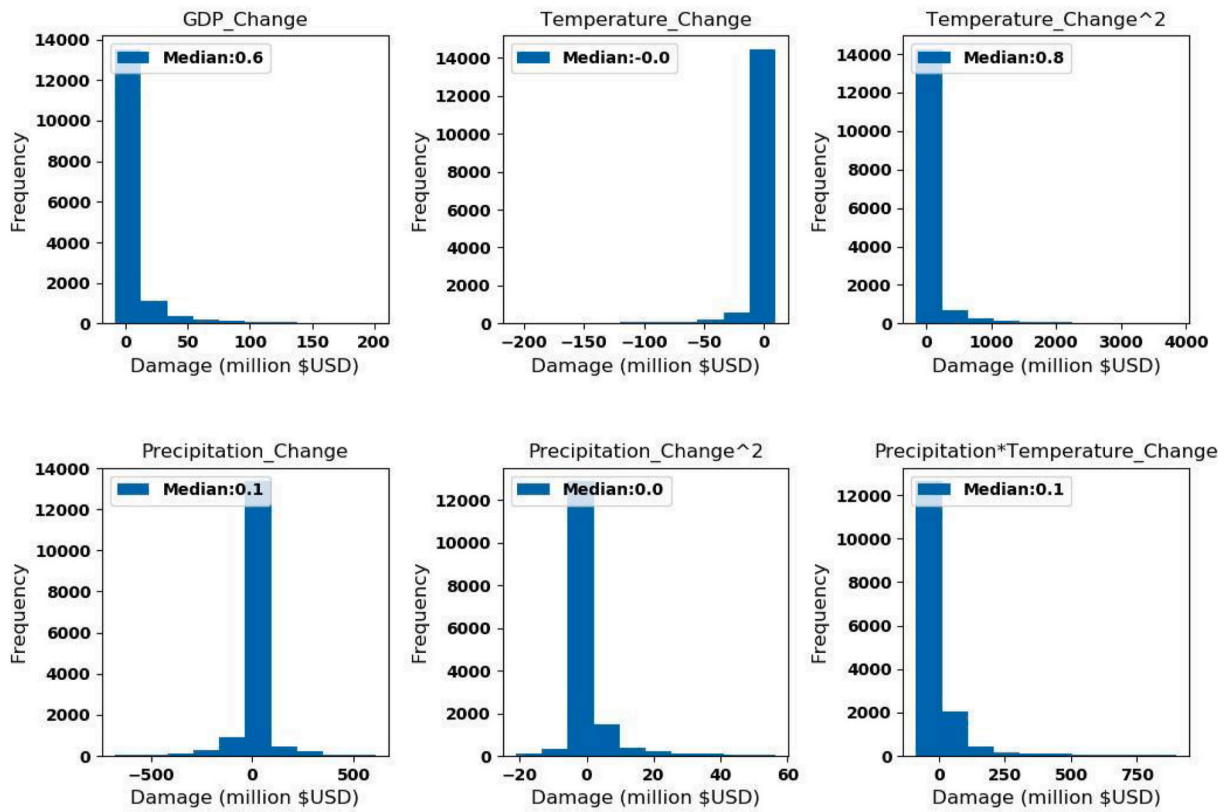**Fig. 14.** Model 6 coefficient distribution: NoStd.
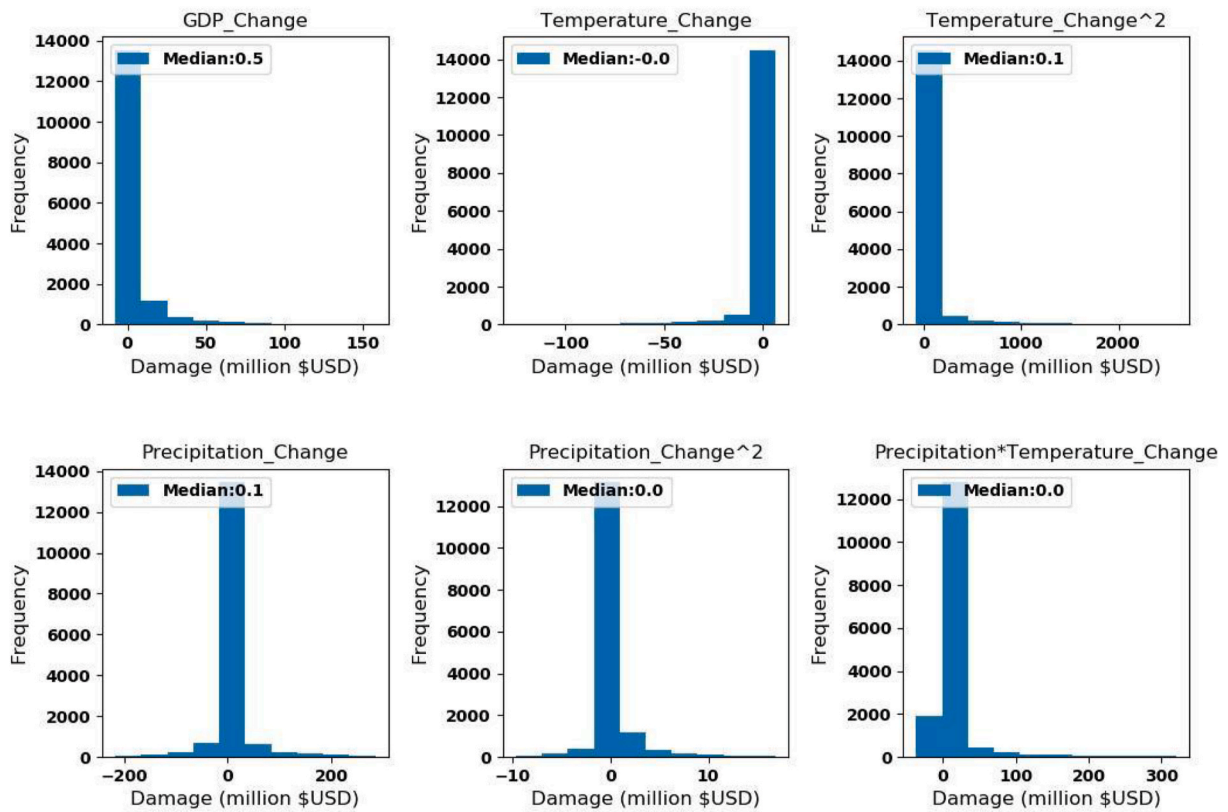
Fig. 15. Model 6 coefficient distribution: BaseHeightStd.

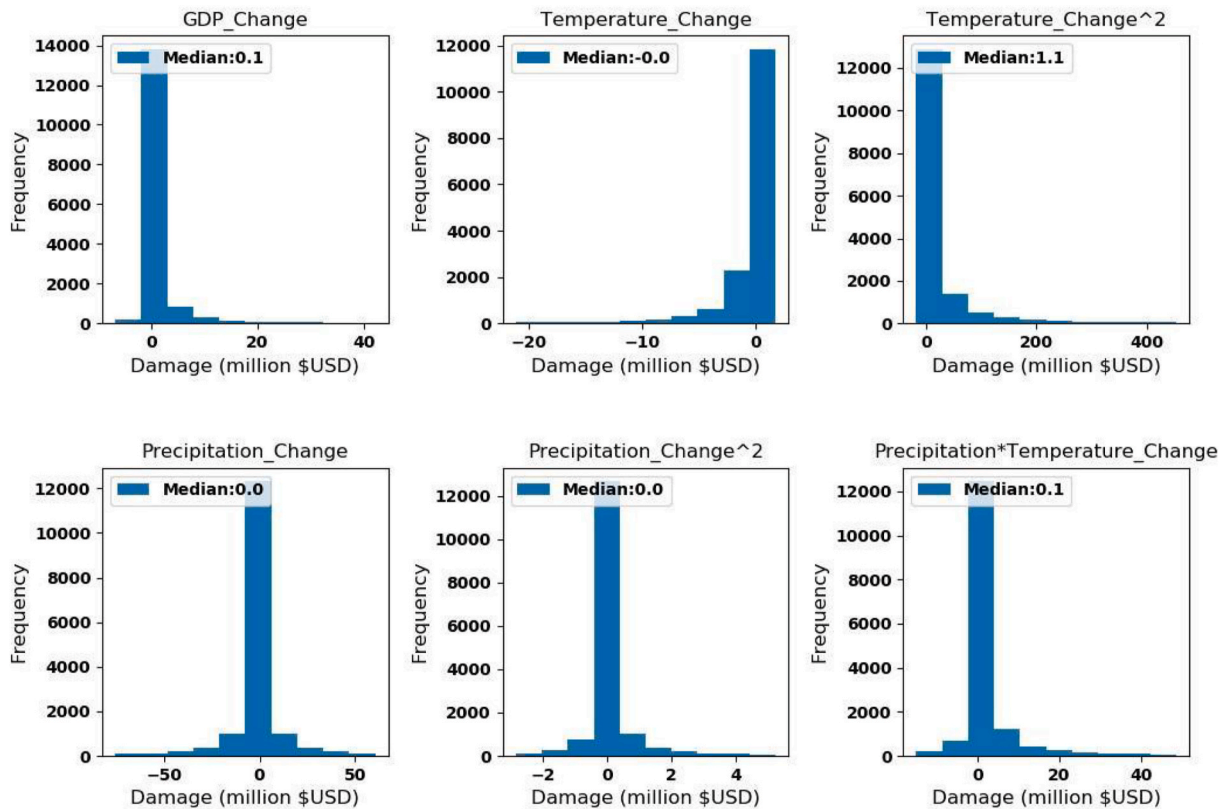**Fig. 16.** Model 6 coefficient distribution: BaseProbStd.

Fig. 17. Model 6 coefficient distribution: OptimalStd.

Table 5
Regression results table for CLIMRISK-RIVER. The coefficients refer to impacts on ΔEAD in millions of dollars (2005, PPP). The effects of temperature and precipitation change grow stronger as the protection standard assumption moves from NoStd towards OptimalStd. However, the effect of ΔGDP on total damage decreases dramatically with improved protection standards, indicating the reduction in river flood vulnerability.

Coefficient					P-value			
Variable	Mean	2.5%	50%	97.5%	Mean	2.5%	50%	97.5%
Nostd								
β_{GDP}	−80.84	−21.65	2.34	345.61	0.002	0	0	0
β_T	−31.62	−272.64	0.08	76.51	0.007	0	0	0.001
β_T^2	7.95	−9.16	0	59.76	0.010 5	0	0	0.038
β_p	1.57	−5.89	0.02	19.99	0.011	0	0	0.052
β_p^2	0.04	−0.46	0	0.8	0.012	0	0	0.098
β_{P*T}	0.9	−3.13	0	9.84	0.011	0	0	0.069
NRMSE (OUT)	1.44	0	0	0.4	# Observations (cells): 16503			
Adj. R^2 (IN)	0.83	0.53	0.86	0.97				
BaseHeightStd								
β_{GDP}	−92.02	−7.61	0.57	201.75	0.003	0	0	0
β_T	−29.82	−198.53	0	14.55	0.009	0	0	0.027
β_T^2	6.62	−2.26	0	35.58	0.012	0	0	0.079
β_p	0.02	−6.66	0	6.19	0.012	0	0	0.091
β_p^2	0.05	−0.22	0	0.56	0.011	0	0	0.057
β_{P*T}	1	−0.89	0	8.89	0.010	0	0	0.045
NRMSE (OUT)	4.5	0	0	0.64	# Observations (cells): 16503			
Adj. R^2 (IN)	0.7	0.25	0.75	0.91				
BaseProbStd								
β_{GDP}	−96.43	−7.23	0.53	158.39	0.002	0	0	0
β_T	−16.22	−117.83	0	14.16	0.007	0	0	0.002
β_T^2	3.64	−1.75	0	23.36	0.010	0	0	0.045
β_p	0.1	−2.14	0	3.08	0.013	0	0	0.119
β_p^2	0.01	−0.1	0	0.17	0.014	0	0	0.158
β_{P*T}	0.44	−0.44	0	3.19	0.014	0	0	0.139
NRMSE (OUT)	3.34	0	0	0.43	#Observations (cells): 16502			
Adj. R^2 (IN)	0.81	0.36	0.85	0.98				
OptimalStd								
β_{GDP}	−131.87	−5.73	0.1	42.19	0.004	0	0	0

(*continued on next page*)

Table 5 (*continued*)

Coefficient					P-value			
Variable	Mean	2.5%	50%	97.5%	Mean	2.5%	50%	97.5%
β_T	−2.2	−3.49	0	4.57	0.009	0	0	0.018
β_T^2	0.63	−0.45	0	1.43	0.012	0	0	0.084
β_p	0.02	−0.43	0	0.59	0.014	0	0	0.141
β_p^2	0.01	−0.03	0	0.04	0.013	0	0	0.136
β_{P*T}	0.12	−0.14	0	0.39	0.013	0	0	0.106
NRMSE (OUT)	4.62	0	0	0.67	*# Observations (cells):* 16503			
Adj. R^2 (IN)	0.66	0.2	0.7	0.91				

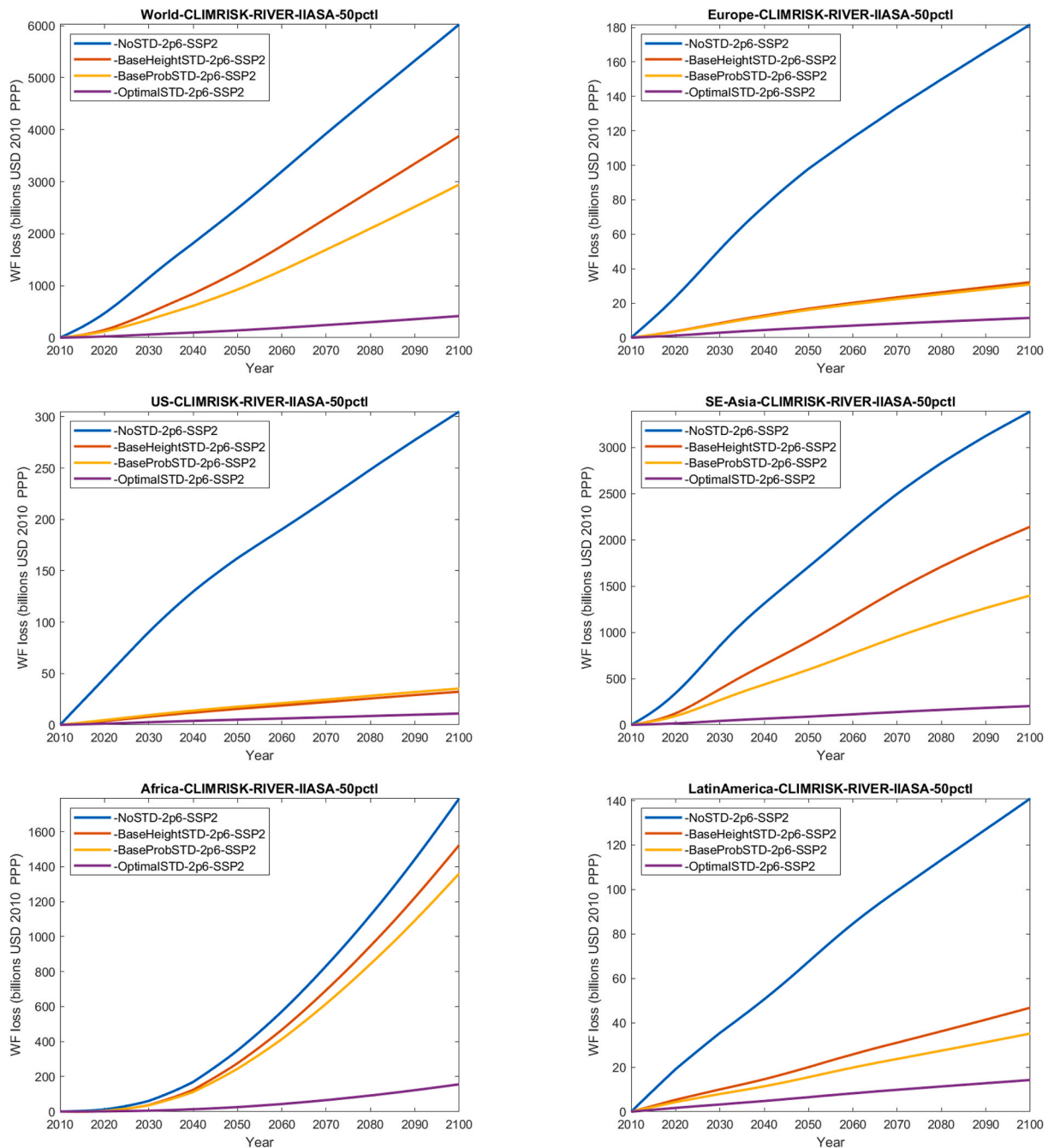## Appendix C. BaseProbSTD and NoSTD results

Fig. 18. Annual ΔEAD in CLIMRISK-RIVER under different protection standards, RCP 2.6 and SSP2 scenario combinations.

Appendix D. Model forecasting performance

NRMSE: Introduction

To evaluate the forecasting performance of the CLIMRISK-RIVER model, we use a statistical method of normalized root mean squared error (NRMSE). First, we compute the within-sample NRMSE by normalizing the root mean squared error (RMSE, Eq. (15)) with the mean value of the observed response variable (Eq. (16)).

To compute the out-of-sample NRMSE statistic for each cell, we run a five-fold stratified cross validation check where we split the data into four stratified training sets and one test set, each subset containing points from a single ESM. Next, we evaluate the out-of-sample RMSE on the test-fold. We repeat the process with a different training-test split set until every fold has been used in testing exactly once. Finally, the mean RMSE value across all five folds is taken and is normalized using the mean value of observed response variable (Eq. (16)) to yield the NRMSE (Eq. (17)).

$$RMSE = \sqrt{\frac{\sum_{n=1}^{N}(\Delta EAD_{GF} - \Delta EAD_{CL-RV})^2}{N}} \qquad (15)$$

$$\Delta \overline{EAD}_{GF} = \sqrt{\frac{\sum_{n=1}^{N}\Delta EAD_{GF_n}}{N}} \qquad (16)$$

$$NRMSE = \frac{RMSE}{\Delta \overline{EAD}_{GF}} \qquad (17)$$

where $\Delta \overline{EAD}_{GF}$ is the mean value of all the ΔEAD_{GF} observations used to fit the damage function for a particular cell. The reason for this normalization is that it gives a more intuitive interpretation of the RMSE by indicating how large the forecasting error is relative to the mean ΔEAD_{GF} observed in GLOFRIS.

NRMSE: Results

In this section, we compare the performance of Models 3 and 6 as potential candidates for CLIMRISK-RIVER. Fig. 19 presents the out-of-sample predictions[20] for the two models of interest. For the estimates of the remaining models, please refer to Fig. 20 and 21.

---

[20] The out-of-sample predictions, labelled as OUT, refer to stratified 5-fold cross validated RMSE estimates normalized using the mean value of the response variable.
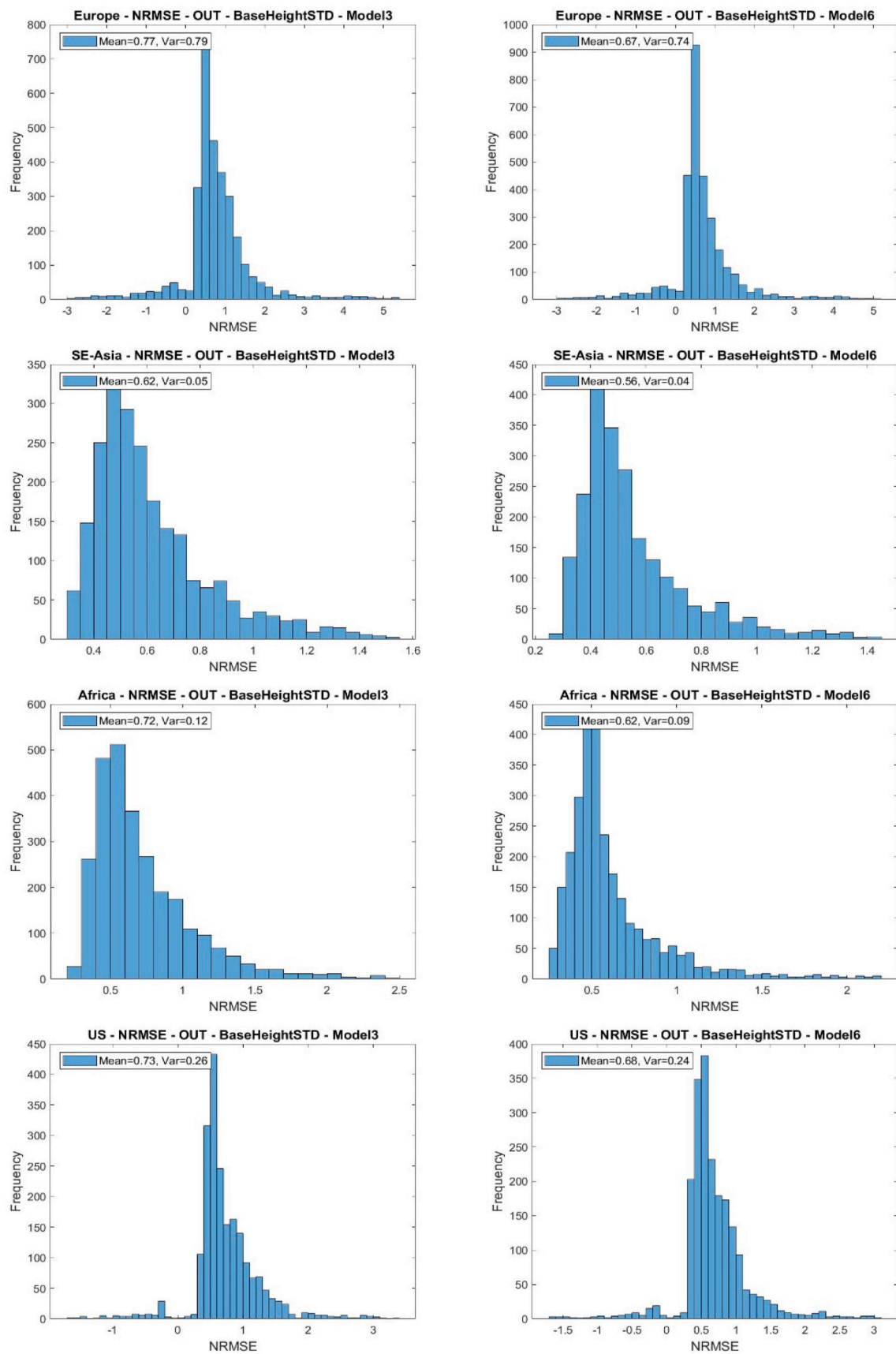
Fig. 19. Forecasting performance of Models 3 and 6: The CLIMRISK-RIVER Model 6 (right panel) has a better forecasting performance than Model 3 (left panel) as measured by out-of-sample NRMSE for presented regions.
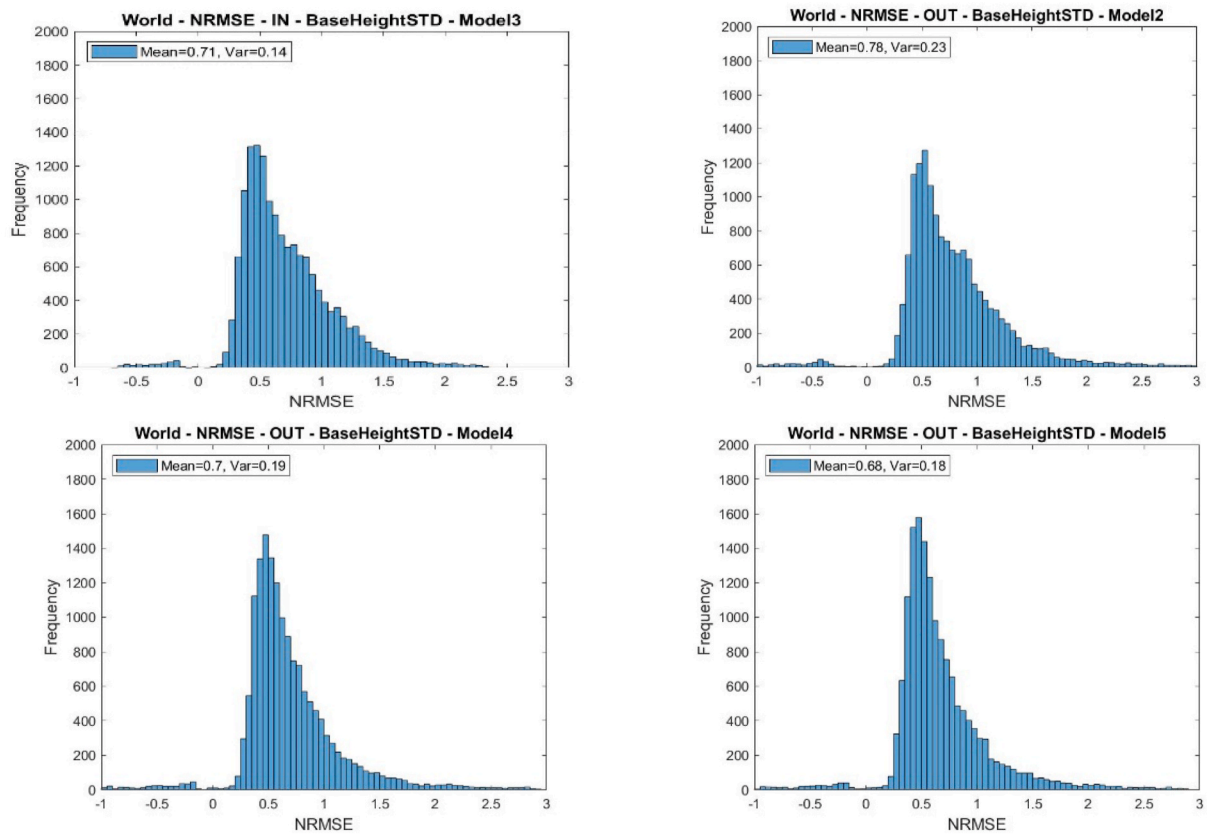
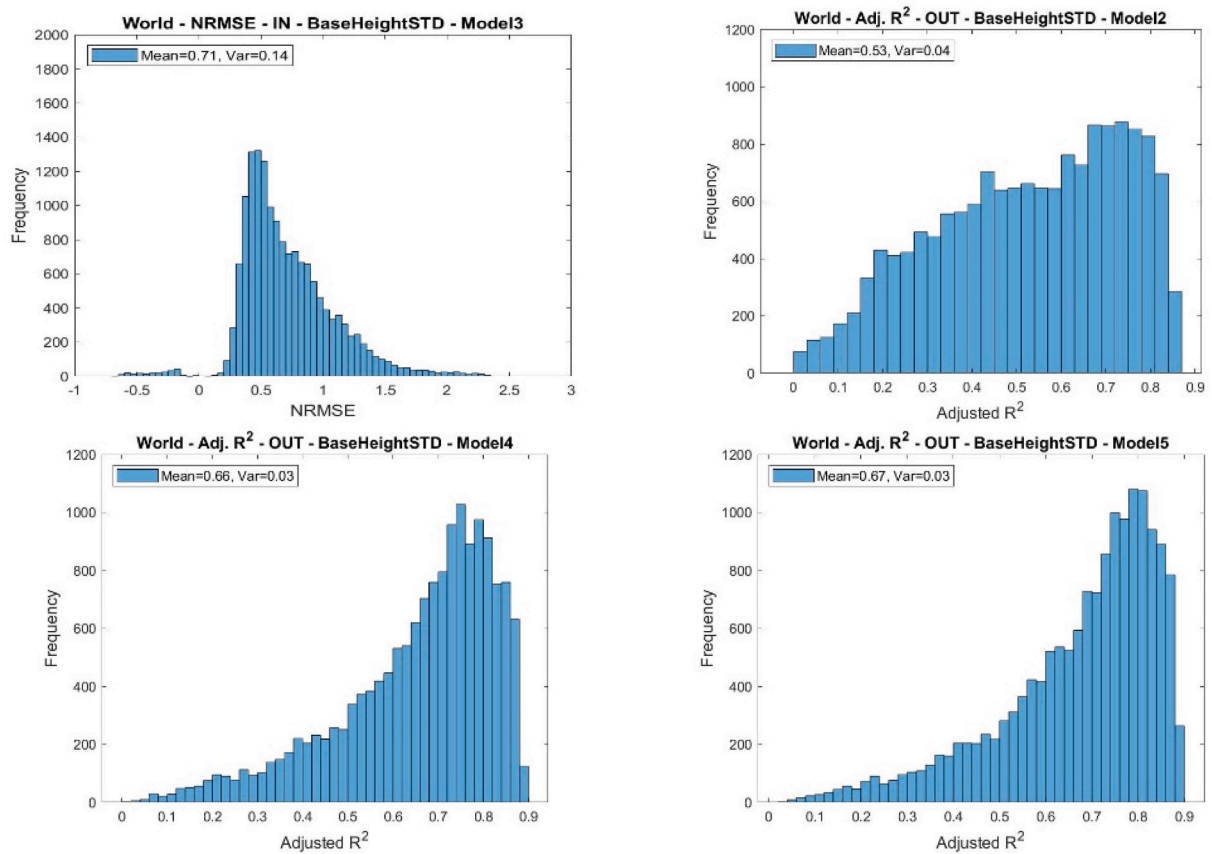**Fig. 20.** Out-of-sample NRMSE for alternative model candidates.

Fig. 21. Out-of-sample adjusted R^2 for alternative model candidates.

Appendix E. Computational performance considerations

Due to the large amount of data required for processing in CLIMRISK, various improvements to performance of the model have been made. The gridded nature of both the flood and climate damage data is suitable for parallel processing. Two API's for parallel processing have been used in the model:

- *Multiprocessing* library in Python which is able to get around the global interpreter lock (GIL), allowing computations to be split into many processes which can be run concurrently, utilizing the full potential of a multi-core system.
- *PyCUDA* library in Python which utilizes the potential of a Graphical Processing Unit (GPU)present in the system. The cellular architecture of a GPU makes solving relatively simple operations over a large grid convenient and fast. Please note that an nVIDIA GPU with CUDA support is required.

References

Anthoff, D., Tol, R.S.J., 2014. The climate framework for uncertainty, negotiation and distribution (FUND), technical description, version 3.9, 26, [Online]. Available. Www.Fund-Model.Org, 1-69. http://www.fund-model.org/versions.

Barker, T., 2007. And others, "Climate change 2007: an assessment of the intergovernmental panel on climate change. Change 446 (November), 12–17.

Bosetti, V., Massetti, E., Tavoni, M., Dec. 2007. The WITCH model: structure, baseline, solutions. SSRN Electron. J. https://doi.org/10.2139/ssrn.960746.

Botzen, W.J.W., Deschenes, O., Sanders, M., Jun. 2019. The economic impacts of natural disasters: a review of models and empirical studies. Rev. Environ. Econ. Pol. https://doi.org/10.1093/reep/rez004.

Bouwman, A.F., Kram, T., Klein Goldewijk, K., 2006. Integrated modelling of global environmental change. An Overv. IMAGE 2 (4), 225–228.

Crespo Cuaresma, J., Jan. 2017. Income projections for climate change research: a framework based on human capital dynamics. Global Environ. Change 42, 226–236. https://doi.org/10.1016/J.GLOENVCHA.2015.02.012.

de Bruin, K.C., Dellink, R.B., Tol, R.S.J., Jul. 2009. AD-DICE: an implementation of adaptation in the DICE model. Climatic Change 95 (1–2), 63–81. https://doi.org/10.1007/s10584-008-9535-5.

Dellink, R., Chateau, J., Lanzi, E., Magné, B., Jan. 2017. Long-term economic growth projections in the shared socioeconomic Pathways. Global Environ. Change 42, 200–214. https://doi.org/10.1016/J.GLOENVCHA.2015.06.004.

Diaz, D., Moore, F., 2017. Quantifying the economic risks of climate change. Nat. Clim. Change 7 (11), 774–782. https://doi.org/10.1038/nclimate3411.

Dobbs, R., Smit, S., Remes, J., Manyika, J., Roxburgh, C., Restrepo, A., 2011. Urban world: mapping the economic power of cities. McKinsey Glob. Inst. 62.

Dumas, P., Ha-Duong, M., Apr. 2013. Optimal growth with adaptation to climate change. Climatic Change 117 (4), 691–710. https://doi.org/10.1007/s10584-012-0601-7.

Estrada, F., Botzen, W.J.W., 2018. Economic Impacts and Risks of Climate Change and Benefits of Current Climate Negotiations. Working paper.

Estrada, F., Botzen, W.J.W., Tol, R.S.J., 2017. A global economic assessment of city policies to reduce climate change impacts. Nat. Clim. Change 7 (6), 403–406. https://doi.org/10.1038/nclimate3301.

Farmer, J.D., Hepburn, C., Mealy, P., Teytelboym, A., 2015. A third wave in the economics of climate change. Environ. Resour. Econ. 62 (2), 329–357. https://doi.org/10.1007/s10640-015-9965-2.

Grübler, A., et al., Sep. 2007. Regional, national, and spatially explicit scenarios of demographic and economic change based on SRES. Technol. Forecast. Soc. Change 74 (7), 980–1029. https://doi.org/10.1016/J.TECHFORE.2006.05.023.

Hope, C.W., 2011. The PAGE09 integrated assessment model: a technical description, 4.

Jongman, B., et al., 2015. Declining vulnerability to river floods and the global benefits of adaptation. Proc. Natl. Acad. Sci. Unit. States Am. 112 (18), E2271–E2280.

Karl, T.R., Diaz, H.F., Kukla, G., Nov. 1988. Urbanization: its detection and effect in the United States climate record. J. Clim. 1 (11), 1099–1123. https://doi.org/10.1175/1520-0442(1988)001<1099:uidaei>2.0.co;2.

Knutti, R., 2010. The end of model democracy? Climatic Change 102 (3), 395–404. https://doi.org/10.1007/s10584-010-9800-2.

Kravitz, B., Lynch, C., Hartin, C., Bond-Lamberty, B., May 2017. "Exploring precipitation pattern scaling methodologies and robustness among CMIP5 models," Geosci. Model Dev 10 (5), 1889–1902. https://doi.org/10.5194/gmd-10-1889-2017.

Kuik, O., 2017. A Simple River Floods Damage Model for the Fund Model. Amsterdam.

Kundzewicz, Z.W., Pińskwar, I., Brakenridge, G.R., 2013. "Large floods in Europe, 1985–2009. Hydrol. Sci. J. 58 (1), 1–7. https://doi.org/10.1080/02626667.2012.745082.

Leimbach, M., Kriegler, E., Roming, N., Schwanitz, J., Jan. 2017. "Future growth patterns of world regions – a GDP scenario approach. Global Environ. Change 42, 215–225. https://doi.org/10.1016/j.gloenvcha.2015.02.005.

Lynch, C., Hartin, C., Bond-Lamberty, B., Kravitz, B., May 2017. An open-access CMIP5 pattern library for temperature and precipitation: description and methodology. Earth Syst. Sci. Data 9 (1), 281–292. https://doi.org/10.5194/essd-9-281-2017.

Meinshausen, M., Raper, S.C.B.B., Wigley, T.M.L.L., 2011. Emulating coupled atmosphere-ocean and carbon cycle models with a simpler model, MAGICC6–Part 1: model description and calibration. Atmos. Chem. Phys. 11 (4), 1417–1456. https://doi.org/10.5194/acp-11-1417-2011.

Meinshausen, M., et al., Nov. 2011. The RCP greenhouse gas concentrations and their extensions from 1765 to 2300. Climatic Change 109 (1), 213–241. https://doi.org/10.1007/s10584-011-0156-z.

Mills, G., 2014. Urban climatology: history, status and prospects. Urban Clim. 10 (P3), 479–489. https://doi.org/10.1016/j.uclim.2014.06.004.

Munich, R.E., Kron, W., Schuck, A., 2014. Topics Geo: Natural Catastrophes 2013: Analyses, Assessments, Positions. Munchener Ruckversicherungs-Gesellschaft.

Nordhaus, W.D., 1992. "The 'DICE' Model: Background and Structure of a Dynamic Integrated Climate-Economy Model of the Economics of Global Warming.

Nordhaus, W.D., 2013. The Climate Casino : Risk, Uncertainty, and Economics for a Warming World.

Nordhaus, W.D., 2014. A Question of Balance: Weighing the Options on Global Warming Policies. Yale University Press.

Nordhaus, W.D., 2017. Revisiting the social cost of carbon. Proc. Natl. Acad. Sci. Unit. States Am. 114 (7), 1518–1523. https://doi.org/10.1073/pnas.1609244114.

Nordhaus, W.D., Yang, Z., 1996. A regional dynamic general-equilibrium model of alternative climate-change strategies. JSTOR Am. Econ. Rev. 86 (4), 741–765 [Online]. Available. https://www.jstor.org/stable/2118303.

Oke, T.R., 1973. City size and the urban heat island. Atmos. Environ. 7 (8), 769–779. https://doi.org/10.1016/0004-6981(73)90140-6.

Rao, S., et al., 2008. IMAGE and MESSAGE Scenarios Limiting GHG Concentration to Low Levels.

Re, M., 2004. Megacities-Megarisks: Trends and Challenges for Insurance and Risk Management. Münchener Rückversicherungs-Gesellschaft, Munich.

Riahi, K., et al., Jan. 2017. The Shared Socioeconomic Pathways and their energy, land use, and greenhouse gas emissions implications: an overview. Global Environ. Change 42, 153–168. https://doi.org/10.1016/J.GLOENVCHA.2016.05.009.

Schleussner, C.F., et al., Aug. 25, 2016. Science and policy characteristics of the Paris Agreement temperature goal. Nat. Clim. Change 6 (9), 827–835. https://doi.org/10.1038/nclimate3096. Nature Publishing Group.

Scussolini, P., et al., 2016. FLOPROS: an evolving global database of flood protection standards. Nat. Hazards Earth Syst. Sci. 16 (5), 1049–1061. https://doi.org/10.5194/nhess-16-1049-2016.

Stern, N., 2008. The Economics of Climate Change 98 (2).

Stern, N., 2013. The structure of economic modeling of the potential impacts of climate change: grafting gross underestimation of risk onto already narrow science models. J. Econ. Lit. 51 (3), 838–859. https://doi.org/10.1257/jel.51.3.838.

Stocker, T.F., et al., 2013. Climate Change 2013 the Physical Science Basis Working Group I Contribution to the Fifth Assessment Report of the Intergovernmental Panel on Climate Change.

Sutanudjaja, E., et al., 2018. PCR-GLOBWB 2: a 5 arc-minute global hydrological and water resources model. Geosci. Model Dev. Discuss. (GMDD) 2018, 1–41.

Tebaldi, C., Arblaster, J.M., Feb. 2014. Pattern scaling: its strengths and limitations, and an update on the latest model simulations. Climatic Change 122 (3), 459–471. https://doi.org/10.1007/s10584-013-1032-9.

Tiggeloven, T., et al., Apr. 2020. Global-scale benefit-cost analysis of coastal flood adaptation to different flood risk drivers using structural measures. Nat. Hazards Earth Syst. Sci. 20 (4), 1025–1044. https://doi.org/10.5194/nhess-20-1025-2020.

Tol, R.S.J., 2008. The social cost of carbon. In: The Oxford Handbook of the Macroeconomics of Global Warming.

Tol, R.S.J., 2018. The economic impacts of climate change. Rev. Environ. Econ. Pol. 4–25. https://doi.org/10.1093/reep/rex027.

van den Bergh, J.C.J.M., Botzen, W.J.W., 2014. A lower bound to the social cost of CO2 emissions. Nat. Clim. Change. https://doi.org/10.1038/nclimate2135.

Van Huijstee, J., van Bemmel, B., Bouwman, A.F.A., van Rijn, F., 2018. Towards an urban preview: modelling future urban growth with 2UP background report. Accessed: Nov. 22, 2018. [Online]. Available. www.pbl.nl/en.

van Vuuren, D.P., Carter, T.R., 2014. Climate and socio-economic scenarios for climate change research and assessment: reconciling the new with the ol. Climatic Change 122 (3), 415–429. https://doi.org/10.1007/s10584-013-0974-2.

Ward, P.J., et al., 2013. Assessing flood risk at the global scale: model setup, results, and sensitivity. Environ. Res. Lett. 8 (4), 44019.

Ward, P.J., et al., Aug. 2015. Usefulness and limitations of global flood risk models. Nat. Clim. Change 5 (8), 712–715. https://doi.org/10.1038/nclimate2742.

Ward, P.J., et al., 2017. A global framework for future costs and benefits of river-flood protection in urban areas. Nat. Clim. Change 7 (9), 642–646. https://doi.org/10.1038/nclimate3350.

Weedon, G.P., et al., Oct. 2011. Creation of the WATCH forcing data and its use to assess global and regional reference crop evaporation over land during the twentieth century. J. Hydrometeorol. 12 (5), 823–848. https://doi.org/10.1175/2011JHM1369.1.

Weigel, A.P., Knutti, R., Liniger, M.A., Appenzeller, C., Aug. 2010. Risks of model weighting in multimodel climate projections. J. Clim. 23 (15), 4175–4191. https://doi.org/10.1175/2010JCLI3594.1.

Winsemius, H.C., Van Beek, L.P.H., Jongman, B., Ward, P.J., Bouwman, A.F., 2012. "A framework for global river flood risk assessments," *Hydrol*. Earth Syst. Sci. 17 (5), 1871–1892. https://doi.org/10.5194/hess-17-1871-2013.

Winsemius, H.C., et al., Apr. 2016. Global drivers of future river flood risk. Nat. Clim. Change 6 (4), 381–385. https://doi.org/10.1038/nclimate2893.